Heliyon 10 (2024) e28890

Contents lists available at ScienceDirect

Heliyon

journal homepage: www.cell.com/heliyon

Research article

Gudermannian neural network procedure for the nonlinear prey-predator dynamical system

Hafsa Alkaabi [a], Noura Alkarbi [a], Nouf Almemari [a], Salem Ben Said [a,*], Zulqurnain Sabir [a,b]

[a] Department of Mathematical Sciences, College of Science, United Arab Emirates University, P. O. Box 15551, Al Ain, United Arab Emirates
[b] Department of Computer Science and Mathematics, Lebanese American University, Beirut, Lebanon

A R T I C L E I N F O

Keywords:
Nonlinear predator-prey system
Gudermannian neural networks
Interior-point algorithm
Genetic algorithm
Numerical computing

A B S T R A C T

The present study performs the design of a novel Gudermannian neural networks (GNNs) for the nonlinear dynamics of prey-predator system (NDPPS). The process of GNNs is applied using the global and local search approaches named as genetic algorithm and interior-point algorithms, i.e., GNNs-GA-IPA. An error-based merit function is constructed using the NDPPS and its initial conditions and then optimized by the hybrid of GA-IPA. Six cases of the NDPPS using the variable coefficients have been presented and the correctness is observed through the overlapping of the obtained and Runge-Kutta reference results. The results of the NDPPS have been performed between 0 and 5 using the step size 0.02. The graph of absolute error are performed around 10^{-06} to 10^{-08} to check the consistency of the proposed GNNs-GA-IPA. The statistical analysis based minimum, median and semi-interquartile ranges have been performed for both predator and prey dynamics of the model. Moreover, the investigations through the statistical operators are performed to validate the reliability of the obtained outcomes based on multiple trials.

1. Introduction

The nonlinear dynamics of the predator-prey system (NDPPS) is discovered few centuries ago by Vito Volterra and Alfred Lotka in the start of 20th century, which is often called Lokta-Volterra system [1]. The NDPPs is one of the mathematical models that is used to define the dynamics of a biological system having two interacting species: a predator and a prey species. Several biological designs are expressed by using the nonlinear differential equations, e.g., HIV infection model, SITR model based on the COVID-19, infection/-treatment system, inflammatory processes of atherosclerosis, dengue fever system and mosquito dispersal model [2–5]. The mathematical form of the model is achieved from the relationship of two kinds of animals, foxes, and rabbits. The clover is eaten by the rabbits and the rabbits are eaten by the foxes. The number of rabbits increase only when the number of foxes reduces and vice versa [6]. This decreasing/increasing conduct of these types of animals represents the nonlinear NDPPS. The structure of prey and predators has an excellent history in the mathematical ecology due to the universal worth and implications [7]. The general form of the model is written as [8–10]:

* Corresponding author.
E-mail addresses: 202109025@uaeu.ac.ae (H. Alkaabi), 202114648@uaeu.ac.ae (N. Alkarbi), 201902140@uaeu.ac.ae (N. Almemari), salem.bensaid@uaeu.ac.ae (S. Ben Said), zulqurnains.abir@lau.edu.lb (Z. Sabir).

https://doi.org/10.1016/j.heliyon.2024.e28890
Received 8 June 2023; Received in revised form 12 March 2024; Accepted 26 March 2024
Available online 2 April 2024

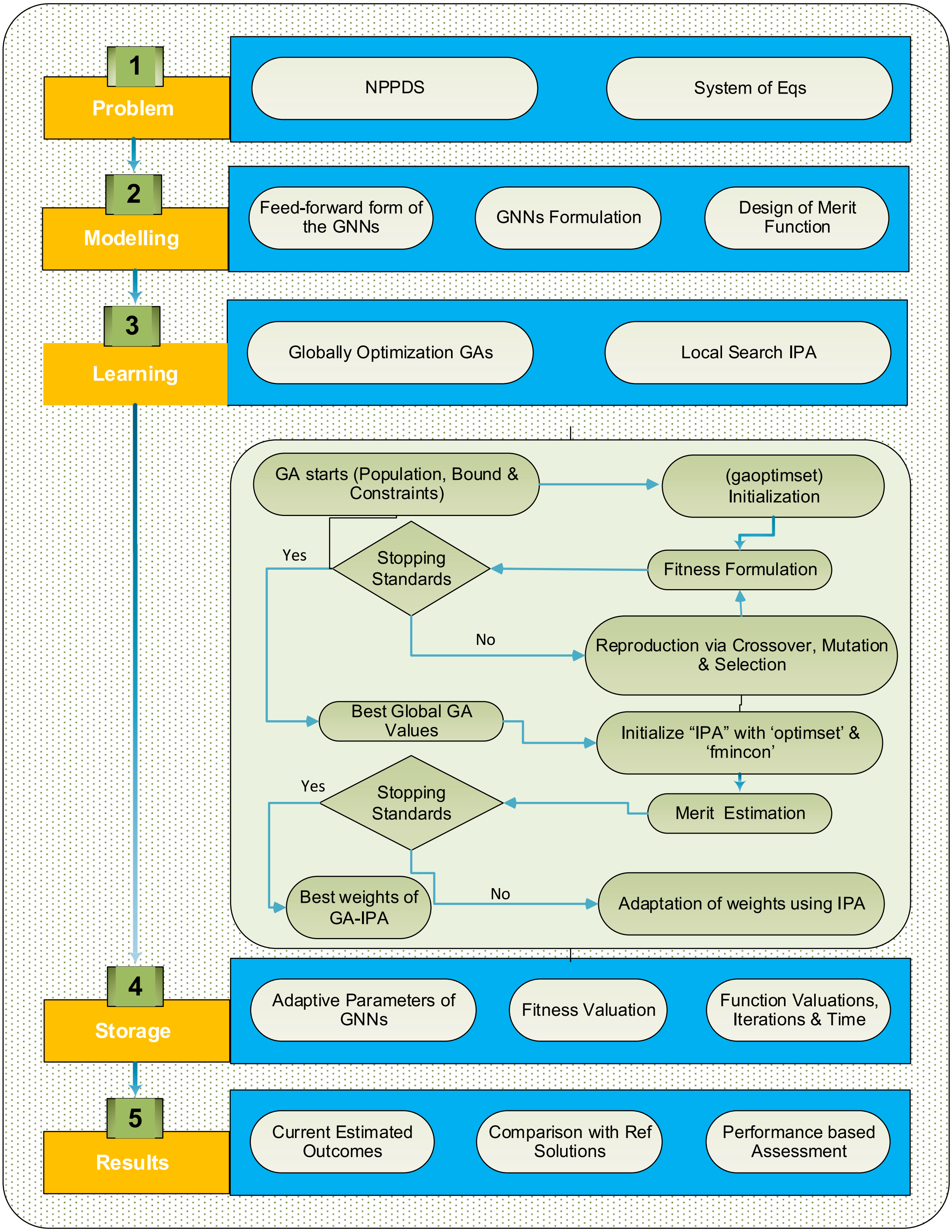

Fig. 1. Graphic representations of GNNs-GA-IPA for solving the NDPPM.

Table 1
Pseudocode using GNNs-GA-IPA for the NDPPS.

GA start
Inputs:
The chromosome signified with same entries of the network as:
$\boldsymbol{W} = [\boldsymbol{W}_p, \boldsymbol{W}_q]$, for $\boldsymbol{W}_p = [\boldsymbol{n}_p, \boldsymbol{w}_p, \boldsymbol{c}_p]$ and $\boldsymbol{W}_q = [\boldsymbol{n}_q, \boldsymbol{w}_q, \boldsymbol{c}_q]$. Where
$\boldsymbol{n}_p = [n_{p,1}, n_{p,2}, \ldots, n_{p,u}], \boldsymbol{w}_p = [w_{p,1}, w_{p,2}, \ldots, w_{p,u}], \boldsymbol{c}_p = [c_{p,1}, c_{p,2}, \ldots, c_{p,u}]$
$\boldsymbol{n}_q = [n_{q,1}, n_{q,2}, \ldots, n_{q,u}],\ \boldsymbol{w}_q = [w_{q,1}, w_{q,2}, \ldots, w_{q,u}],\ \boldsymbol{c}_q = [c_{q,1}, c_{q,2}, \ldots, c_{q,u}].$
Population: The set of chromosomes is written as:
$\boldsymbol{P} = [(\boldsymbol{W}_{p1}, \boldsymbol{W}_{p2}, \ldots, \boldsymbol{W}_{pn}), (\boldsymbol{W}_{q1}, \boldsymbol{W}_{q2}, \ldots, \boldsymbol{W}_{qn})]$, $[\boldsymbol{W}_{pi}, \boldsymbol{W}_{qi}] = [(\boldsymbol{n}_{qi}, \boldsymbol{w}_{qi}, \boldsymbol{c}_{qi}), (\boldsymbol{n}_{qi}, \boldsymbol{w}_{qi}, \boldsymbol{c}_{qi})]$
Output: The best GA values are signified as $\boldsymbol{W}_{GB}$
Initialization: Produce $\boldsymbol{W}$ vector using the real values to indicate a. chromosome. Adjust the $\boldsymbol{W}$ *vector* to form an initial $\boldsymbol{P}$. *Regulate* the Generation and declarations values using the gaoptimset & GA.
Fitness Formulation
Obtained ζ_{Fit} for $\boldsymbol{W}$ in $\boldsymbol{P}$ using Eqs (5-8)
Terminating Criteria
Execution of the scheme stops if
ζ_{Fit}=10^{-19}, Executions= 30, StallGenLimit=80, TolCon=TolFun=10^{-20}, PopulationSize=180, other=defaults values
Move to **[storage]**, when meets the terminating criteria.
Rank
Rank each $\boldsymbol{W}$ in population $\boldsymbol{P}$ via ζ_{Fit} values.
Store
$\boldsymbol{W}_{GB}$ with the time, ζ_{Fit}, generation, and current GA trials.
End the GA process

Start the IPA process
Inputs: Primary weights are $\boldsymbol{W}_{GB}$
Output: GA-IPA is the Weight vector, i.e., $\boldsymbol{W}_{GA-IPA}$
Initialization: $\boldsymbol{W}_{GB}$ is applied as an initial point, generations & bounded assignments.
Termination criteria: End the adaptation process, if meet, [ζ_{Fit}=10^{-20}], [Iterations= 900], [TolCon =TolFun= TolX = 10^{-22}], and [MaxFunEvals= 2690000].
While [Terminate]
Fitness Evaluation: To assess ζ_{Fit} of $\boldsymbol{W}$ for Eqs (6-8)
Fine tuning: Apply [fmincon] routine. Update the factors of $\boldsymbol{W}$ for each iteration of IPA and calculate ζ_{Fit} of enhanced $\boldsymbol{W}$ for Eqs (6-8)
Store
Store $\boldsymbol{W}_{GA-IPA}$, iterations, ζ_{Fit}, time, and function counts.
End of IPA process

$$
\begin{cases}
p'(\tau) = p(\tau)(a - bq(\tau)), \\
q'(\tau) = -q(t)(c - dp(\tau)), \\
p(0) = \alpha_1, q(0) = \alpha_2,
\end{cases}
\tag{1}
$$

where a, b, c and d present the constant parameters, α_1, α_2 indicate the initial conditions (ICs), whereas $p(\tau)$ and $q(\tau)$ show the predators and the prey at the time τ. The NDPPS is represented by the innovator's work of Lotka-Volterra and further Holling [11] discussed three types of functional reactions. When the population of prey is high, there is sufficient food for the predators due to this the predator population increase. While the population of predator enhances, they devour more prey leading to a reduction in the prey population. On the other hand, the decrement in the prey population lessens and the food accessible for the predators by producing the predator population to decrease. The cycle replicates as the influence of predator and prey perform over time. The model based on the Lotka-Volterra undertakes the simplistic relations and does not interpret for the factors, like competition, spatial distribution, and environmental intricacies. The model forecasts cyclical fluctuations in populations that cannot reflect the dynamics of real-world precisely. The research community implemented both modeling and simulation in the process of biomathematics for solving the nonlinear systems using the analytical or numerical approaches [12–14].

Recently, numerous schemes have been established to perform the solutions of the NDPPS, e.g., differential transformation approach, Runge–Kutta method, Adomian decomposition technique, Homotopy approach, finite element, Sumudu decomposition scheme, Adams implicit method, reduced fractional differential transformation approach and confidence domain technique [15–21]. All these approaches have their own applicability and limitations. However, the computing stochastic numerical solvers using the Gudermannian neural networks (GNNs) have never been implemented before to solve the NDPPS. Recently, the artificial neural networks (ANNs) using the stochastic standards have successfully applied for the linear/nonlinear systems arising in various submissions [22–28]. Some current applications of these solvers are SITR model based on coronavirus [29,30], nonlinear third kind of singular models [31,32], monkeypox transmission system [33], heat conduction model [34], periodic differential model [35], influenza disease mathematical system [36], water pollution model [37], and SIR nonlinear dengue fever model [38]. These suggestions not only provide the significance of computing solvers, but also stimulated the authors to form a consistent, stable, and precise scheme to solve the NDPPS. Some novel features of the present study are given as:

- The design of GNNs is presented efficiently using the global and local search approaches for solving the model (1).
- The approximate outcomes of the NDPPM are accessible for better understanding to operate the proposed stochastic numerical solvers.
- GNNs is presented as a novel design based on the layer structures to get the reliable, precise, and effective solutions to solve the NDPPS.
- Execution of GNNs together with the optimization of evolutionary heuristic is provided with a quick local search IPA to find an accurate, consistent, and robust numerical measures of the NDPPS.
- The reliable overlapping solutions with desired outcomes, enhance the precision and stability of the stochastic computing GNNs-GA-IPA solver.
- Authentication of the GNNs-GA-IPA solver is implemented on different performances to verify the reliability of the scheme.
- The merits of the GNNs-GA-IPA solvers include comprehensible structure, inclusive applications, and ease in implementation to handle the complex and stiff NDPPS.

The rest of the paper parts are as follows: Sect 2 shows the designed GNNS-GA-IPA methodology. Sect 3 shows the mathematical form of the statistical operator. Sect 4 provides the comprehensive results and discussions. Sect 5 shows the concluding remarks along with the future research directions.

2. Methodology

The methodology of GNNs-GA-IPA is presented by constructing an objective function that is optimized by using the hybridization of GA-IPA. The graphical plots of the GNNs-GA-IPA are provided in Fig. 1.

2.1. Design of GNNs

The mathematical designs of NDPPM signified in Eq (1) are specified with the art of feed forward GNNs in terms of estimated results along with the 1st derivatives as:

$$[\widehat{p}(\tau), \widehat{q}(\tau)] = \left[\sum_{i=1}^{u} n_{p,i} M\left(w_{p,i}\tau + c_{p,i}\right), \sum_{i=1}^{u} n_{q,i} M\left(w_{q,i}\tau + c_{q,i}\right)\right], \tag{2}$$

$$[\widehat{p}'(\tau), \widehat{q}'(\tau)] = \left[\sum_{i=1}^{u} n_{p,i} M'\left(w_{p,i}\tau + c_{p,i}\right), \sum_{i=1}^{u} n_{q,i} M'\left(w_{q,i}\tau + c_{q,i}\right)\right],$$

where u represents the neurons and $[\boldsymbol{n}, \boldsymbol{w}, \boldsymbol{c}]$ indicates the unknown weights, i.e., $\boldsymbol{W} = [\boldsymbol{n}, \boldsymbol{w}, \boldsymbol{c}]$ as: $\boldsymbol{W} = [\boldsymbol{W}_p, \boldsymbol{W}_q]$, for $\boldsymbol{W}_p = [\boldsymbol{n}_p, \boldsymbol{w}_p, \boldsymbol{c}_p]$ and $\boldsymbol{W}_q = [\boldsymbol{n}_q, \boldsymbol{w}_q, \boldsymbol{c}_q]$, where

$$\begin{aligned} \boldsymbol{n}_p &= \left[n_{p,1}, n_{p,2}, \ldots, n_{p,u}\right], \boldsymbol{w}_p = \left[w_{p,1}, w_{p,2}, \ldots, w_{p,u}\right], \boldsymbol{c}_p = \left[c_{p,1}, c_{p,2}, \ldots, c_{p,u}\right] \\ \boldsymbol{n}_q &= \left[n_{q,1}, n_{q,2}, \ldots, n_{q,u}\right], \boldsymbol{w}_q = \left[w_{q,1}, w_{q,2}, \ldots, w_{q,u}\right], \boldsymbol{c}_q = \left[c_{q,1}, c_{q,2}, \ldots, c_{q,u}\right]. \end{aligned}$$

The Gudermannian function (GF) is mathematically written as:

$$M(\tau) = 2\left(\tan^{-1}[\exp(\tau)] - \pi\right). \tag{3}$$

The updated form of Eq (2) using the above form is given as:

Table 2
Statistical analysis of case I based on NDPPM.

τ	Predator $p(\tau)$ values for Case I			Prey $q(\tau)$ values for Case I		
	Min	Med	SIR	Min	Med	SIR
0	3.862115E-10	4.753992E-07	5.762575E-08	1.117240E-08	2.832141E-07	7.293358E-06
0.2	3.538723E-07	1.472043E-05	1.235683E-05	4.659493E-07	5.903591E-06	8.200841E-06
0.4	3.786991E-06	1.791489E-05	1.333671E-05	3.934612E-08	9.251085E-06	7.553462E-06
0.6	5.315175E-08	9.669985E-06	5.264596E-06	4.892819E-07	1.283220E-05	6.735321E-06
0.8	3.924328E-08	8.814256E-06	4.710730E-06	3.758982E-07	1.644359E-05	8.982586E-06
1	3.164897E-07	1.238877E-05	1.047215E-05	2.144528E-06	1.800621E-05	1.140547E-05
1.2	4.429477E-07	1.053564E-05	9.949862E-06	1.505542E-06	1.613240E-05	1.553570E-05
1.4	2.076737E-07	1.143450E-05	1.486095E-05	2.980184E-06	1.681279E-05	1.291342E-05
1.6	4.591873E-07	1.677306E-05	1.255546E-05	1.843547E-06	2.066410E-05	1.314849E-05
1.8	1.078762E-06	1.518644E-05	8.483996E-06	2.962434E-07	1.739666E-05	1.508649E-05
2	1.423055E-06	1.841045E-05	6.837257E-06	5.034076E-07	1.372643E-05	1.467651E-05
2.2	3.660290E-06	1.570294E-05	5.789332E-06	1.171325E-06	1.755706E-05	1.386127E-05
2.4	5.421323E-06	9.228399E-06	6.062688E-06	5.565641E-07	2.425363E-05	1.235852E-05
2.6	6.826832E-07	1.088219E-05	9.236946E-06	5.920743E-07	3.393977E-05	2.083996E-05
2.8	1.550790E-06	1.557491E-05	1.309380E-05	2.451516E-07	4.065908E-05	2.897944E-05
3	5.937599E-07	1.608346E-05	1.609629E-05	2.111561E-06	4.443068E-05	3.561299E-05
3.2	7.137758E-07	1.579010E-05	1.206633E-05	3.102793E-06	4.967394E-05	3.597183E-05
3.4	1.012155E-06	1.122000E-05	1.016936E-05	3.232298E-06	5.764117E-05	3.910716E-05
3.6	3.622182E-07	9.439083E-06	7.640099E-06	2.928389E-07	5.917500E-05	4.235735E-05
3.8	1.160174E-07	1.507296E-05	1.042784E-05	2.412972E-06	5.997494E-05	4.123139E-05
4	4.942364E-07	1.866090E-05	1.253657E-05	2.415529E-06	6.275880E-05	4.552426E-05
4.2	1.675414E-06	2.089697E-05	1.240150E-05	5.801215E-07	6.632460E-05	5.053649E-05
4.4	1.203168E-06	1.271830E-05	5.047078E-06	1.383294E-06	6.202957E-05	5.338892E-05
4.6	2.819279E-07	8.383533E-06	6.953005E-06	3.233800E-06	6.335493E-05	5.901543E-05
4.8	9.419300E-07	1.606773E-05	1.268952E-05	2.318142E-06	6.630768E-05	6.220771E-05
5	9.723745E-07	1.224575E-05	7.388747E-06	4.471022E-06	6.980361E-05	6.102351E-05

$$
\begin{aligned}
[\widehat{p}(\tau),\widehat{q}(\tau)] &= \left[\sum_{i=1}^{u} n_{p,i}\left(2\left(\tan^{-1}e^{\left(w_{p,i}\tau+c_{p,i}\right)}-\pi\right)\right),\sum_{i=1}^{u} n_{q,i}\left(2\left(\tan^{-1}e^{\left(w_{q,i}\tau+c_{q,i}\right)}-\pi\right)\right)\right],\\
[\widehat{p}'(\tau),\widehat{q}'(\tau)] &= \left[\sum_{i=1}^{u} 2n_{p,i}w_{p,i}\left(\frac{e^{\left(w_{p,i}\tau+c_{p,i}\right)}}{1+\left(e^{\left(w_{p,i}\tau+c_{p,i}\right)}\right)^2}\right),\sum_{i=1}^{u} 2n_{q,i}w_{q,i}\left(\frac{e^{\left(w_{q,i}\tau+c_{q,i}\right)}}{1+\left(e^{\left(w_{q,i}\tau+c_{q,i}\right)}\right)^2}\right)\right],
\end{aligned}
\tag{4}
$$

To solve the NDPPS, a merit function is designed as:

$$\zeta_{Fit}=\zeta_{Fit-1}+\zeta_{Fit-2}+\zeta_{Fit-3}, \tag{5}$$

where ζ_{Fit-1} and ζ_{Fit-2} are the merit functions related to predator $p(\tau)$ and prey $q(\tau)$. While ζ_{Fit-3} is designed based on the ICs of the NDPPM, given as:

$$\zeta_{Fit-1}=\frac{1}{N}\sum_{i=1}^{N}\left(\widehat{p}'_i-a\widehat{p}_i+b\widehat{p}_i\widehat{q}_i\right)^2, \tag{6}$$

$$\zeta_{Fit-2}=\frac{1}{N}\sum_{i=1}^{N}\left(\widehat{q}'_i+c\widehat{q}_i-d\widehat{p}_i\widehat{q}_i\right)^2, \tag{7}$$

$$\zeta_{Fit-3}=\frac{1}{2}\left(\left(\widehat{p}_0-\alpha_1\right)^2+\left(\widehat{q}_0-\alpha_2\right)^2\right), \tag{8}$$

where $Nh=1, \widehat{p}_i=\widehat{p}(\tau_i), \widehat{q}_i=\widehat{q}(\tau_i), \tau_i=ih$.

To find the solutions of the NDPPS given in Eq (1), a merit function $\zeta_{Fit}\rightarrow 0$ and the obtained outcomes becomes as $[\widehat{p}(\tau),\widehat{q}(\tau)]\rightarrow[p(\tau), q(\tau)]$.

2.2. Optimization: GA-IPA

The comprehensive detail of the optimization schemes using the GA-IPA is presented in this section.

GA is known as a global search technique, which applies to the evolutionary theories based on the process of natural genetic growth in human realities. It is operated randomly as an effectual intelligent search approach. To accomplish the best system consequences, GA is implemented along with some tools like mutation, selection, and crossover. It is used in frequent submissions like as wellhead

Table 3
Statistical analysis of case II based on NDPPM.

τ	Predator $p(\tau)$ values for Case II			Prey $q(\tau)$ values for Case II		
	Min	Med	SIR	Min	Med	SIR
0	5.008800E-09	1.112844E-07	1.552875E-07	7.353584E-11	4.534702E-08	9.442531E-08
0.2	3.262579E-07	5.638121E-06	4.526192E-06	1.204292E-07	1.118300E-05	7.203376E-06
0.4	4.248723E-08	7.407955E-06	3.281623E-06	7.490602E-07	9.811468E-06	7.671452E-06
0.6	1.313915E-06	4.231614E-06	1.948672E-06	1.874431E-07	7.223265E-06	4.835878E-06
0.8	1.882073E-07	3.651817E-06	3.190989E-06	1.772773E-07	5.721512E-06	7.702854E-06
1	2.623148E-07	3.621244E-06	4.308735E-06	9.173342E-07	4.910360E-06	9.107154E-06
1.2	6.213624E-07	7.181857E-06	4.761089E-06	1.731374E-07	9.058990E-06	5.219196E-06
1.4	1.018764E-06	7.760123E-06	3.061722E-06	6.100369E-08	7.516021E-06	7.927778E-06
1.6	5.249086E-07	5.516891E-06	2.764693E-06	1.577090E-06	1.141747E-05	7.035096E-06
1.8	6.519645E-07	3.909457E-06	2.298650E-06	3.951674E-07	1.609519E-05	8.609970E-06
2	4.215408E-07	7.507757E-06	5.334665E-06	1.849840E-06	1.504049E-05	7.896640E-06
2.2	2.858655E-07	7.136868E-06	8.390601E-06	1.787328E-06	1.148423E-05	1.022923E-05
2.4	4.517074E-07	6.641240E-06	8.088683E-06	6.119716E-07	9.039369E-06	1.015637E-05
2.6	9.779275E-07	5.826505E-06	6.074694E-06	1.110786E-06	6.834258E-06	8.038987E-06
2.8	1.209414E-07	6.075253E-06	4.597354E-06	3.314065E-07	7.959488E-06	6.470556E-06
3	7.476873E-07	7.221680E-06	4.170024E-06	3.285702E-07	1.131439E-05	9.087173E-06
3.2	1.873894E-08	5.661582E-06	3.861220E-06	3.591071E-09	1.241079E-05	8.548621E-06
3.4	4.359561E-07	7.656275E-06	3.656138E-06	1.102739E-06	1.260295E-05	4.884570E-06
3.6	6.034048E-08	9.693866E-06	4.181668E-06	5.537298E-07	1.248986E-05	9.518502E-06
3.8	1.588823E-06	7.587079E-06	4.472973E-06	2.123241E-06	1.336606E-05	1.028988E-05
4	1.190404E-07	7.601477E-06	4.529107E-06	1.908818E-06	1.460229E-05	1.255392E-05
4.2	1.726978E-08	5.944656E-06	2.776767E-06	2.234096E-07	1.587528E-05	1.372080E-05
4.4	1.293547E-06	5.491054E-06	4.652431E-06	5.099135E-07	1.572613E-05	8.638296E-06
4.6	4.138243E-07	5.645582E-06	3.764790E-06	9.810269E-07	1.770041E-05	9.517704E-06
4.8	1.280804E-06	6.261936E-06	4.306802E-06	1.155873E-07	1.423849E-05	1.239241E-05
5	8.908584E-07	6.825243E-06	3.364016E-06	7.479883E-08	1.509413E-05	1.025695E-05

back pressure control system [39], bank lending decisions [40], cancer microarray high-dimensional datasets [41], fuzzy clustering for bankruptcy prediction [42], quality features in gas tungsten arc welding progression [43], intrusion detection system [44], path planning based dynamic areas [45], automotive diesel engine calibration [46], novel synthetical index control [47] and damage assessment in structures [48].

IPA is identified as a local search technique that is implemented to the convex and constrained/unconstrained models. The optimal results of GA are used as an initial input in the process of IPA. Therefore, the hybridization of GA with the IPA is performed to solve this model. Recently, IPA is applied in the brittle/ductile breakage [49], multistage nonlinear nonconvex programs [50], simulation of aircraft parts riveting [51], nonlinear second-order cone programming [52], large-scale convex optimization [53], and efficient single objective optimization problem [54]. The mutual strength of GNNs-GA-IPA is used to present the solutions of six different cases of NDPPS described in Table 1.

2.3. *Limitations of the proposed scheme*

GNN is one of the types of the ANNs, which uses the GF as an activation function (AF). GNNs has widely implemented like other neural networks, like convolutional or feed-forward neural networks. Therefore, less resources and pre-trained models are available in the literature based on the GNNs. The implementation of the GNNs need particular knowledge of the GF along with its specified properties. As compared to other AF, one can face more challenges to apply the GF due to deep architectures for solving a problem. In the detailed investigations, the gradient vanishing commonly performed in the deep neural networks can become prominent while using the GF as an activation function. Like many other types of neural networks, GNNs also contain black-box systems like other neural networks, which become more difficult to understand that how the performance of the model attains its predictions.

3. Performance measures

In this section, the performances based on the mean absolute error (MAE), Theil inequality coefficient (TIC) and error in Nash–Sutcliffe efficiency (ENCE) are presented to solve the NDPPM, which is mathematically given as:

$$[MAD_p, MAD_q] = \left[\frac{1}{v}\sum_{i=1}^{v}|(p_i - \widehat{p}_i)|, \frac{1}{v}\sum_{i=1}^{v}|q_i - \widehat{q}_i|\right], \tag{9}$$

Table 4
Statistical analysis of case III based on NDPPM.

τ	Predator $p(\tau)$ values for Case III			Prey $q(\tau)$ values for Case III		
	Min	Med	SIR	Min	Med	SIR
0	6.102845E-10	1.382514E-07	1.043503E-06	2.905489E-09	4.927976E-07	7.387680E-07
0.2	2.793402E-06	6.660428E-06	8.285138E-06	1.986000E-06	7.332012E-06	5.861538E-06
0.4	8.822753E-07	6.639282E-06	8.591212E-06	1.268752E-06	1.207324E-05	1.018073E-05
0.6	2.892979E-07	5.508133E-06	4.184406E-06	8.328638E-07	1.099461E-05	1.164624E-05
0.8	5.023357E-07	5.228295E-06	5.313517E-06	1.744554E-06	5.374242E-06	1.391871E-05
1	3.380172E-07	7.034302E-06	7.377308E-06	9.898399E-08	6.814628E-06	8.525320E-06
1.2	2.716554E-08	6.840374E-06	5.570498E-06	5.496160E-07	8.097834E-06	5.810794E-06
1.4	3.935954E-07	1.083030E-05	9.292120E-06	3.960852E-07	6.410629E-06	7.645798E-06
1.6	1.076495E-06	1.606804E-05	1.118102E-05	3.265774E-08	6.249256E-06	6.553615E-06
1.8	2.288658E-06	9.410082E-06	5.962861E-06	3.318808E-07	6.865617E-06	1.030210E-05
2	2.842418E-07	7.302170E-06	7.698912E-06	7.934009E-07	1.105572E-05	1.379532E-05
2.2	7.503335E-07	9.997499E-06	1.061398E-05	6.425076E-07	1.323206E-05	1.100589E-05
2.4	7.190957E-07	9.286138E-06	1.231647E-05	5.202351E-07	1.309404E-05	8.139225E-06
2.6	6.354342E-07	1.011235E-05	6.604675E-06	4.022354E-07	1.097410E-05	1.033741E-05
2.8	1.552675E-06	1.428085E-05	1.213126E-05	4.788800E-07	1.027876E-05	1.188718E-05
3	2.930617E-06	1.289457E-05	1.106712E-05	1.273840E-06	9.339889E-06	9.088005E-06
3.2	1.399963E-06	9.250251E-06	1.323723E-05	3.237309E-07	9.287108E-06	1.047863E-05
3.4	4.012515E-07	1.403804E-05	1.475525E-05	8.790020E-07	9.161949E-06	1.303224E-05
3.6	3.562772E-06	1.600694E-05	1.557112E-05	1.164919E-06	1.107249E-05	1.666544E-05
3.8	2.787506E-06	1.577009E-05	1.440599E-05	5.599566E-07	1.489827E-05	1.691613E-05
4	7.854533E-07	1.199192E-05	9.178607E-06	6.553686E-07	1.291635E-05	1.446978E-05
4.2	5.938660E-07	9.081474E-06	8.596976E-06	1.296894E-06	1.061922E-05	1.380324E-05
4.4	8.276796E-07	1.003661E-05	1.427491E-05	3.318030E-06	1.307637E-05	9.381622E-06
4.6	1.038890E-06	2.226492E-05	2.113412E-05	3.816466E-07	1.591806E-05	1.161194E-05
4.8	1.956148E-06	2.582541E-05	1.861336E-05	2.994406E-06	1.895589E-05	9.486777E-06
5	1.843173E-06	1.384163E-05	8.010264E-06	2.626453E-06	1.158986E-05	9.054810E-06

$$[\mathrm{TIC}_p, \mathrm{TIC}_q] = \left(\frac{\sqrt{\frac{1}{v}\sum_{i=1}^{v} (p_i - \widehat{p}_i)^2}}{\left(\sqrt{\frac{1}{v}\sum_{i=1}^{v} p_i^2} + \sqrt{\frac{1}{v}\sum_{i=1}^{v} \widehat{p}_i^2}\right)}, \frac{\sqrt{\frac{1}{v}\sum_{i=1}^{v} (q_i - \widehat{q}_i)^2}}{\left(\sqrt{\frac{1}{v}\sum_{i=1}^{v} \widehat{q}_i^2} + \sqrt{\frac{1}{v}\sum_{i=1}^{v} \widehat{q}_i^2}\right)} \right), \tag{10}$$

$$[NSE_p, NSE_q] = \left[\left(1 - \frac{\mathrm{var}(p_i - \widehat{p}_i)}{\mathrm{var}(p_i)}\right) \times 100, \left(1 - \frac{\mathrm{var}(q_i - \widehat{q}_i)}{\mathrm{var}(q_i)}\right) \times 100 \right], \tag{11}$$

where, the ENSE is the error in NSE, written as:

$$[ENSE_p, ENSE_q] = [|ENSE_p - 100|, |ENSE_q - 100|]. \tag{12}$$

4. Results and simulations

In this section, the numerical soundings of NDPPM are expressed using the proposed GNNs-GA-IPA. The reference results through Runge-kutta scheme are presented because of non-availability of exact results. The comparison of the obtained and reference results is presented for solving six dissimilar cases of the NDPPM.

Case I. Consider a NDPPM by taking $a = 0.1, b = 0.014, c = 0.012, d = 0.08$, $\alpha_1 = 3$ and $\alpha_2 = 6$ in system (1) as:

$$\begin{cases} p^{'}(\tau) = 0.1p(\tau) - 0.014p(\tau)q(\tau), \\ q^{'}(\tau) = -0.012q(t) + 0.08p(\tau)q(t), \\ p(0) = 3, q(0) = 6. \end{cases} \tag{13}$$

A merit function for the above system (13) is written as:

$$\zeta_{Fit} = \frac{1}{N}\sum_{i=1}^{N} \left((\widehat{p}^{'}_i - 0.1\widehat{p}_i + 0.014\widehat{p}_i\widehat{q}_i)^2 + (\widehat{q}^{'}_i + 0.012q_i - 0.08\widehat{p}_i\widehat{q}_i)^2 \right) + \frac{1}{2}\left((\widehat{p}_0 - 3)^2 + (\widehat{q}_0 - 6)^2 \right). \tag{14}$$

The optimization performances using the GNNs-GA-IPA are presented to solve the case I of the NDPPM through the hybrid of GA-

Table 5
Statistical analysis of case IV based on NDPPM.

τ	Predator $p(\tau)$ values for Case IV			Prey $q(\tau)$ values for Case IV		
	Min	Med	SIR	Min	Med	SIR
0	5.146572E-11	3.347536E-08	6.097074E-09	5.174243E-10	6.221764E-08	9.944376E-08
0.2	3.133878E-08	3.357916E-06	6.303919E-06	6.220822E-08	8.813173E-06	6.449496E-06
0.4	8.840322E-08	4.683481E-06	6.137619E-06	1.163577E-07	6.274629E-06	4.291497E-06
0.6	4.092191E-07	2.988828E-06	1.343618E-06	7.016866E-09	4.020895E-06	2.133434E-06
0.8	1.132405E-07	1.867068E-06	2.101785E-06	2.046720E-08	6.434399E-06	3.968266E-06
1	1.228935E-08	2.971016E-06	4.674449E-06	5.353914E-07	6.677789E-06	6.103015E-06
1.2	3.078443E-07	3.598155E-06	6.775225E-06	2.522539E-07	5.661515E-06	6.334208E-06
1.4	5.892788E-07	4.884513E-06	6.754135E-06	2.059024E-06	6.952882E-06	5.367382E-06
1.6	1.627437E-07	5.875492E-06	6.093370E-06	6.485204E-07	7.188943E-06	4.124959E-06
1.8	4.056449E-07	5.242023E-06	2.710959E-06	9.544346E-07	6.319047E-06	4.418463E-06
2	2.093922E-07	3.558491E-06	2.220881E-06	6.042182E-08	4.709914E-06	4.397078E-06
2.2	1.048350E-06	5.648498E-06	2.475442E-06	1.026486E-07	4.862631E-06	4.336777E-06
2.4	3.195706E-07	3.970500E-06	3.152927E-06	2.316627E-08	4.407094E-06	3.261003E-06
2.6	6.719844E-08	2.999260E-06	4.761200E-06	8.655298E-07	4.958288E-06	4.070213E-06
2.8	6.948476E-08	3.905695E-06	7.104423E-06	1.136424E-06	5.362303E-06	3.302755E-06
3	2.008526E-07	5.365881E-06	8.380292E-06	3.038629E-07	7.051251E-06	5.135869E-06
3.2	4.500658E-07	6.631641E-06	5.774145E-06	5.103207E-08	7.430237E-06	6.656698E-06
3.4	6.571847E-07	6.714695E-06	4.953089E-06	6.071175E-07	1.016329E-05	6.078245E-06
3.6	2.189791E-06	5.423731E-06	4.232229E-06	8.283654E-07	1.082005E-05	6.058416E-06
3.8	1.076464E-06	5.873495E-06	3.457670E-06	4.944607E-07	1.082175E-05	5.573829E-06
4	4.543826E-07	4.846549E-06	3.611840E-06	2.010862E-06	9.857093E-06	3.427649E-06
4.2	2.382781E-07	5.263746E-06	2.604751E-06	2.090757E-06	7.604877E-06	2.715894E-06
4.4	5.847993E-07	3.893122E-06	4.011173E-06	9.125438E-08	4.015371E-06	4.330921E-06
4.6	7.277924E-07	6.300794E-06	6.669296E-06	4.226404E-07	3.242069E-06	4.777404E-06
4.8	6.396207E-07	6.505096E-06	5.951243E-06	4.849276E-08	4.437113E-06	5.332791E-06
5	1.558387E-07	4.847755E-06	4.845393E-06	1.674083E-07	4.087236E-06	3.981578E-06

IPA for 20 independent trials. The numerical results have been calculated in inputs 0 to 5 along with the 0.02 step size. The set of approximate results based on the parameters $p(\tau)$ and $q(\tau)$ for case I are written as:

$$\begin{aligned}\widehat{p}_{C-I}(\tau) = & -0.4\left(2arc\tan e^{(0.1\tau+0.1)}-\frac{\pi}{2}\right)-1.7\left(2\arctan e^{(-0.2\tau-2)}-\frac{\pi}{2}\right)+0.4\left(2arc\tan e^{(0.4\tau+1)}-\frac{\pi}{2}\right)\\ & +1.1\left(2arc\tan e^{(-0.3\tau+1.8)}-\frac{\pi}{2}\right)+0.3\left(2arc\tan e^{(0.3\tau-0.3)}-\frac{\pi}{2}\right)+0.3\left(2arc\tan e^{(-0.2\tau-0.4)}-\frac{\pi}{2}\right)\\ & +0.8\left(2arc\tan e^{(-0.7\tau-3.2)}-\frac{\pi}{2}\right)+0.3\left(2arc\tan e^{(0.4\,\tau+1.1)}-\frac{\pi}{2}\right)+0.7\left(2arc\tan e^{(0.5\tau+22.1)}-\frac{\pi}{2}\right)\\ & +0.7\left(2arc\tan e^{(-0.6\tau-2.9)}-\frac{\pi}{2}\right),\end{aligned} \tag{15}$$

$$\begin{aligned}\widehat{q}_{C-I}(\tau) = & -3\left(2arc\tan e^{(-0.1\tau-0.8)}-\frac{\pi}{2}\right)-2\left(2arc\tan e^{(-0.1\tau-3.3)}-\frac{\pi}{2}\right)+2.7\left(2arc\tan e^{(0.3\tau-0.8)}-\frac{\pi}{2}\right)\\ & -1.9\left(2arc\tan e^{(-0.1\tau-1.4)}-\frac{\pi}{2}\right)-3.8\left(2arc\tan e^{(-0.3\tau-0.3)}-\frac{\pi}{2}\right)+2.1\left(2arc\tan e^{(0.4\tau+3)}-\frac{\pi}{2}\right)\\ & +3.2\left(2arc\tan e^{(0.1\tau-3.1)}-\frac{\pi}{2}\right)+5.3\left(2arc\tan e^{(3.5\tau-0.5)}-\frac{\pi}{2}\right)-6.8\left(2arc\tan e^{(3.0\tau+0.3)}-\frac{\pi}{2}\right)\\ & +2.9\left(2arc\tan e^{(-7.2\tau+2.8)}-\frac{\pi}{2}\right).\end{aligned} \tag{16}$$

Table 2 shows the statistical analysis of the predator $p(\tau)$ and prey $q(\tau)$ for case I. The values of the Median (Med), Minimum (Min) means the best trials, and semi-interquartile ranges (SIR) for solving the predator $p(\tau)$ and prey $q(\tau)$ indexes based on the NDPPM are provided in Table 2. The Min values authenticates the best trials, while the SIR is one half of the difference of 3rd and 1st quartiles. These values have been calculated in interval 0 and 5 with 0.2 step size. The Min, Med and SIR performances for predator $p(\tau)$ based case I lie as 10^{-06} to 10^{-10}, 10^{-05} to 10^{-08} and 10^{-05} to 10^{-07}, while the Min, Med and SIR prey $q(\tau)$ values for case I are found around 10^{-07} to 10^{-08}, 10^{-05} to 10^{-07} and 10^{-05} to 10^{-06}. These negligible measures indicate the reliability and exactness of proposed solver.

Case II. Consider a NDPPM by using $a = 0.1, b = 0.024, c = 0.012, d = 0.08$, $\alpha_1 = 2$ and $\alpha_2 = 4$ in system (1) as:

$$\begin{cases} p'(\tau) = 0.1p(\tau) - 0.024p(\tau)q(\tau), \\ q'(\tau) = -0.012q(t) + 0.08p(\tau)q(t), \\ p(0) = 2, q(0) = 4. \end{cases} \tag{17}$$

A merit function for the above system (17) is written as:

Table 6
Statistical analysis of case V based on NDPPM.

τ	Predator $p(\tau)$ values for Case V			Prey $q(\tau)$ values for Case V		
	Min	Med	SIR	Min	Med	SIR
0	3.028920E-09	2.370424E-07	2.449041E-07	9.452705E-11	2.304647E-07	4.366170E-07
0.2	2.216000E-06	8.416765E-06	6.701856E-06	8.075714E-07	1.440461E-05	1.356582E-05
0.4	2.325474E-07	1.175285E-05	6.777018E-06	2.213930E-07	1.492973E-05	9.432892E-06
0.6	4.657405E-08	6.757116E-06	3.848047E-06	2.509700E-07	1.196260E-05	6.784959E-06
0.8	6.198788E-07	8.307542E-06	8.502215E-06	5.723321E-07	1.304488E-05	1.061012E-05
1	7.386886E-07	8.494389E-06	7.101620E-06	5.305545E-07	6.690787E-06	1.314288E-05
1.2	1.327672E-07	8.760821E-06	7.982624E-06	1.679225E-07	7.201173E-06	1.293507E-05
1.4	4.695079E-07	9.309609E-06	6.339077E-06	6.882266E-07	9.736647E-06	1.037461E-05
1.6	4.579853E-07	1.170442E-05	8.804390E-06	4.426674E-07	1.287256E-05	1.066106E-05
1.8	9.371088E-08	1.191276E-05	5.015433E-06	1.442111E-06	1.457642E-05	1.157333E-05
2	2.581124E-06	1.228465E-05	7.405479E-06	1.863453E-07	1.785621E-05	1.571477E-05
2.2	1.711395E-06	1.070039E-05	8.119376E-06	4.214106E-07	1.621966E-05	1.497019E-05
2.4	5.548336E-07	1.348483E-05	1.062676E-05	2.056262E-06	1.132096E-05	1.908740E-05
2.6	1.526429E-07	1.136584E-05	1.258253E-05	2.025283E-06	1.076414E-05	1.460466E-05
2.8	1.317135E-07	1.267935E-05	1.141667E-05	1.764111E-06	1.000601E-05	1.296141E-05
3	1.319645E-07	1.547257E-05	1.056211E-05	1.277918E-06	1.055128E-05	1.387363E-05
3.2	4.378046E-07	1.230952E-05	1.363425E-05	3.609173E-07	8.761290E-06	1.004146E-05
3.4	2.170806E-07	1.330534E-05	1.244622E-05	7.131994E-07	1.366630E-05	8.971703E-06
3.6	3.866918E-07	1.588249E-05	6.454983E-06	6.083467E-07	1.461091E-05	1.013259E-05
3.8	1.460289E-06	1.275821E-05	5.542566E-06	6.792111E-07	1.899742E-05	1.186058E-05
4	2.105295E-06	1.061939E-05	7.333879E-06	1.195588E-06	2.134163E-05	1.763870E-05
4.2	1.314841E-06	9.705910E-06	4.390299E-06	8.114635E-07	1.752532E-05	2.120530E-05
4.4	4.796199E-07	1.168821E-05	1.300636E-05	6.526217E-07	1.835578E-05	2.087277E-05
4.6	5.210839E-07	1.702952E-05	2.149081E-05	9.449837E-07	1.932633E-05	2.283498E-05
4.8	2.290120E-06	2.196867E-05	2.175413E-05	1.315623E-06	1.633230E-05	1.999772E-05
5	5.133567E-07	1.594920E-05	1.362595E-05	3.739491E-08	1.766397E-05	2.212974E-05

$$\zeta_{Fit} = \frac{1}{N}\sum_{i=1}^{N}\left(\left(\widehat{p}_i' - 0.1\widehat{p}_i + 0.024\widehat{p}_i\widehat{q}_i\right)^2 + \left(\widehat{q}_i' + 0.012q_i - 0.08\widehat{p}_i\widehat{q}_i\right)^2\right) + \frac{1}{2}\left(\left(\widehat{p}_0 - 2\right)^2 + \left(\widehat{q}_0 - 4\right)^2\right). \tag{18}$$

The optimization performances using the GNNs-GA-IPA to solve the case II based on the NDPPM is obtained through the hybridization of GA-IPA for 20 independent trials. The numerical results have been calculated in inputs 0 to 5 by taking 0.02 step size. The set of approximate results of $p(\tau)$ and $q(\tau)$ for case II are written as:

$$\begin{aligned}\widehat{p}_{C-II}(\tau) = {} & 0.2\left(2arc\tan e^{(0.3\tau-0.1)} - \frac{\pi}{2}\right) - 0.1\left(2arc\tan e^{0.1\tau+0.3)} - \frac{\pi}{2}\right) + 0.7\left(2arc\tan e^{(-0.1\tau-0.3)} - \frac{\pi}{2}\right) \\ & +1.4\left(2arc\tan e^{(0.2\tau+1.3)} - \frac{\pi}{2}\right) + 0.9\left(2arc\tan e^{(-0.2\tau+1.2)} - \frac{\pi}{2}\right) - 0.7\left(2arc\tan e^{(0.1\tau-0.1)} - \frac{\pi}{2}\right) - 0.1\left(2arc\tan e^{(-0.9\tau+0.1)} - \frac{\pi}{2}\right) \\ & -0.3\left(2arc\tan e^{(-0.2\,\tau+0.5)} - \frac{\pi}{2}\right) - 0.3\left(2arc\tan e^{(0.3\tau+0.1)} - \frac{\pi}{2}\right) \\ & +0.1\left(2arc\tan e^{(0.6\tau-0.5)} - \frac{\pi}{2}\right),\end{aligned} \tag{19}$$

$$\begin{aligned}\widehat{q}_{C-II}(\tau) = {} & 2.9\left(2arc\tan e^{(-0.1\tau+0.7)} - \frac{\pi}{2}\right) + 3.1\left(2arc\tan e^{(0.1\tau+1.6)} - \frac{\pi}{2}\right) + 0.8\left(2arc\tan e^{(-0.1\tau+0.6)} - \frac{\pi}{2}\right) \\ & +9.6\left(2arc\tan e^{(-1.3\tau+0.7)} - \frac{\pi}{2}\right) - 2.0\left(2arc\tan e^{(-0.1\tau-1.7)} - \frac{\pi}{2}\right) + 2.5\left(2arc\tan e^{(0.1\tau-0.3)} - \frac{\pi}{2}\right) - 0.1\left(2arc\tan e^{(1.0\tau+1.5)} - \frac{\pi}{2}\right) \\ & +4.2\left(2arc\tan e^{(0.2\tau-1.1)} - \frac{\pi}{2}\right) - 0.1\left(2arc\tan e^{(-0.1\tau-3.1)} - \frac{\pi}{2}\right) - 1.2\left(2arc\tan e^{(0.1\tau-0.3)} - \frac{\pi}{2}\right).\end{aligned} \tag{20}$$

Table 3 indicates the statistical analysis of predator $p(\tau)$ and prey $q(\tau)$ for case II. The values of Min, Med, and SIR for solving the predator $p(\tau)$ and prey $q(\tau)$ indexes are tabulated in Table 3. These values have been calculated in interval 0 and 5. It is seen that the Min, Med and SIR based on the predator $p(\tau)$ for Case II are performed as 10^{-06} to 10^{-09}, 10^{-06} to 10^{-07} and 10^{-05} to 10^{-07}, while the Min, Med and SIR prey $q(\tau)$ values for Case II are found around 10^{-07} to 10^{-11}, 10^{-05} to 10^{-08} and 10^{-05} to 10^{-08}. These reducible performances indicate the reliability and exactness of the proposed scheme.

Case III. Consider a NDPPM by having the values of $a = 0.1, b = 0.034, c = 0.012, d = 0.08$, $\alpha_1 = 1$ and $\alpha_2 = 2$ in system (1) as:

$$\begin{cases} p'(\tau) = 0.1p(\tau) - 0.034p(\tau)q(\tau), \\ q'(\tau) = -0.012q(t) + 0.08p(\tau)q(t), \\ p(0) = 1, q(0) = 2. \end{cases} \tag{21}$$

A merit function for the above system (21) is written as:

$$\begin{aligned}\zeta_{Fit} = & \frac{1}{N}\sum_{i=1}^{N}\left((\widehat{p}'_i - 0.1\widehat{p}_i + 0.034\widehat{p}_i\widehat{q}_i)^2 + (\widehat{q}'_i + 0.012q_i - 0.08\widehat{p}_i\widehat{q}_i)^2\right) \\ & + \frac{1}{2}\left((\widehat{p}_0 - 1)^2 + (\widehat{q}_0 - 2)^2\right).\end{aligned} \tag{22}$$

The optimization performances using the GNNs-GA-IPA are presented in order to solve the 3rd case. The optimization is obtained through the process of GA-IPA by taking 20 independent trials. The numerical results have been calculated in inputs 0 to 5 and by using 0.02 step size. The set of approximate results of $p(\tau)$ and $q(\tau)$ for 3rd case is written as:

$$\begin{aligned}\widehat{p}_{C-III}(\tau) = & -0.1\left(2arc\tan e^{(-0.3\tau-0.1)} - \frac{\pi}{2}\right) + 6.5\left(2arc\tan e^{(-1\tau+1)} - \frac{\pi}{2}\right) - 1.0\left(2arc\tan e^{(-0.9\tau+2.1)} - \frac{\pi}{2}\right) \\ & -0.03\left(2arc\tan e^{(-0.3\tau+1)} - \frac{\pi}{2}\right) + 0.3\left(2arc\tan e^{(-0.5\tau-1.0)} - \frac{\pi}{2}\right) + 1.1\left(2arc\tan e^{(-0.7\tau-1)} - \frac{\pi}{2}\right) \\ & +0.1\left(2arc\tan e^{(0.3\tau-0.2)} - \frac{\pi}{2}\right) + 1.5\left(2arc\tan e^{(0.7\tau+1.2)} - \frac{\pi}{2}\right) + 0.6\left(2arc\tan e^{(-0.2\tau-3.7)} - \frac{\pi}{2}\right) \\ & +0.04\left(2arc\tan e^{(0.2\tau+0.6)} - \frac{\pi}{2}\right),\end{aligned} \tag{23}$$

$$\begin{aligned}\widehat{q}_{C-III}(\tau) = & -0.7\left(2arc\tan e^{(-0.2\tau+2)} - \frac{\pi}{2}\right) + 1.8\left(2arc\tan e^{(0.1\tau+0.5)} - \frac{\pi}{2}\right) + 3.3\left(2arc\tan e^{(-1\tau+0.1)} - \frac{\pi}{2}\right) \\ & +0.5\left(2arc\tan e^{(1.3\tau-0.5)} - \frac{\pi}{2}\right) - 0.1\left(2arc\tan e^{(-0.1\tau+0.8)} - \frac{\pi}{2}\right) + 2.5\left(2arc\tan e^{(0.9\tau-0.1)} - \frac{\pi}{2}\right) - 0.1\left(2arc\tan e^{(3.8\tau+1.2)} - \frac{\pi}{2}\right) \\ & +0.06\left(2arc\tan e^{(1.1\tau-1)} - \frac{\pi}{2}\right) + 0.8\left(2arc\tan e^{(1.5\tau+1.3)} - \frac{\pi}{2}\right) - 0.04\left(2arc\tan e^{(2.6\tau+0.4)} - \frac{\pi}{2}\right).\end{aligned} \tag{24}$$

Table 4 represents the statistical analysis of the predator $p(\tau)$ and prey $q(\tau)$ for case III. The values of Min, Med, and SIR for solving the predator $p(\tau)$ and prey $q(\tau)$ indexes are tabulated in Table 4. These values have been calculated in input 0 and 5 with 0.2 step size. The Min, Med and SIR performances for the predator $p(\tau)$ based Case III are calculated as 10^{-06} to 10^{-10}, 10^{-05} to 10^{-07} and 10^{-05} to 10^{-06}, while the Min, Med and SIR prey $q(\tau)$ values for Case III are found around 10^{-06} to 10^{-09}, 10^{-05} to 10^{-07} and 10^{-06} to 10^{-07}. These small measures indicate the reliability and exactness of proposed technique.

Case IV. Consider a NDPPM using the values $a = 0.1, b = 0.014, c = 0.012, d = 0.01$, $\alpha_1 = 1$ and $\alpha_2 = 3$. The NDPPM based system (1) is updated as:

$$\begin{cases} p'(\tau) = 0.1p(\tau) - 0.014p(\tau)q(\tau), \\ q'(\tau) = -0.012q(t) + 0.01p(\tau)q(t), \\ p(0) = 1, q(0) = 3. \end{cases} \tag{25}$$

A merit function for the above system (25) is written as:

$$\begin{aligned}\zeta_{Fit} = & \frac{1}{N}\sum_{i=1}^{N}\left((\widehat{p}'_i - 0.1\widehat{p}_i + 0.014\widehat{p}_i\widehat{q}_i)^2 + (\widehat{q}'_i + 0.012q_i - 0.01\widehat{p}_i\widehat{q}_i)^2\right) \\ & + \frac{1}{2}\left((\widehat{p}_0 - 1)^2 + (\widehat{q}_0 - 3)^2\right).\end{aligned} \tag{26}$$

The optimization performances using the GNNs-GA-IPA to solve the case IV based on the NDPPM are obtained through GA-IPA for 20 independent trials. The numerical results have been calculated in inputs 0 to 5 using 0.02 step size. The set of approximate results for $p(\tau)$ and $q(\tau)$ for case IV are written as:

$$\begin{aligned}\widehat{p}_{C-IV}(\tau) = & 0.03\left(2arc\tan e^{(0.2\tau+0.01)} - \frac{\pi}{2}\right) + 0.4\left(2arc\tan e^{(0.3\tau+1.8)} - \frac{\pi}{2}\right) + 0.1\left(2arc\tan e^{(0.1\tau-0.03)} - \frac{\pi}{2}\right) \\ & -0.1\left(2arc\tan e^{(0.3\tau+0.5)} - \frac{\pi}{2}\right) - 0.03\left(2arc\tan e^{(-0.8\tau-0.6)} - \frac{\pi}{2}\right) - 0.1\left(2arc\tan e^{(0.3\tau-2.6)} - \frac{\pi}{2}\right) \\ & +0.06\left(2arc\tan e^{(0.1\tau+0.05)} - \frac{\pi}{2}\right) - 0.01\left(2arc\tan e^{(2.0\tau+1.2)} - \frac{\pi}{2}\right) + 0.8\left(2arc\tan e^{(0.03\tau+0.6)} - \frac{\pi}{2}\right) \\ & +0.07\left(2arc\tan e^{(0.9\tau+1.8)} - \frac{\pi}{2}\right),\end{aligned} \tag{27}$$

Table 7
Statistical analysis of case VI based on NDPPM.

τ	Predator $p(\tau)$ values for Case VI			Prey $q(\tau)$ values for Case VI		
	Min	Med	SIR	Min	Med	SIR
0	5.459784E-10	1.037465E-07	2.961860E-07	1.626332E-09	9.477435E-08	4.693939E-07
0.2	7.549614E-07	6.126193E-06	5.714379E-06	2.870339E-07	5.762313E-06	9.786169E-06
0.4	1.401225E-06	8.213898E-06	9.463948E-06	3.279725E-07	1.368010E-05	1.983629E-05
0.6	5.664826E-07	5.902477E-06	8.761107E-06	1.581592E-06	1.446574E-05	1.195310E-05
0.8	1.506791E-07	3.749453E-06	1.102075E-05	1.077302E-06	1.118649E-05	1.219787E-05
1	7.552769E-08	5.006191E-06	5.402363E-06	9.052437E-07	1.156208E-05	1.165313E-05
1.2	5.092977E-07	2.461799E-06	4.944091E-06	1.591962E-06	1.255989E-05	1.493380E-05
1.4	1.541268E-07	9.302398E-06	7.626980E-06	8.612379E-07	1.104072E-05	2.036130E-05
1.6	2.963101E-08	1.052731E-05	1.030543E-05	6.608754E-07	1.418376E-05	1.714006E-05
1.8	5.974500E-07	8.491083E-06	1.236110E-05	9.850420E-07	1.509233E-05	2.067814E-05
2	4.452718E-07	8.980536E-06	6.301570E-06	1.482971E-07	1.805299E-05	2.130126E-05
2.2	1.420251E-06	8.442136E-06	1.059196E-05	2.434697E-06	1.931944E-05	1.651831E-05
2.4	2.025776E-07	9.485948E-06	1.702753E-05	7.791784E-07	2.535302E-05	1.805992E-05
2.6	3.404297E-07	1.202374E-05	1.200394E-05	2.789978E-06	2.520210E-05	2.061561E-05
2.8	1.497275E-06	9.318763E-06	9.450343E-06	1.090920E-06	2.344684E-05	2.574355E-05
3	2.879485E-07	8.419053E-06	5.643687E-06	1.407121E-06	2.341758E-05	3.722472E-05
3.2	3.412985E-09	8.923277E-06	7.248601E-06	7.303865E-07	2.243849E-05	3.777321E-05
3.4	1.942660E-07	6.628915E-06	8.923983E-06	6.643521E-07	2.130528E-05	3.601731E-05
3.6	7.686355E-07	7.733192E-06	5.824026E-06	1.655298E-06	2.036620E-05	3.194300E-05
3.8	6.070989E-07	1.069788E-05	6.162451E-06	2.596981E-07	2.196888E-05	2.817894E-05
4	8.300522E-07	1.148875E-05	5.200637E-06	4.661458E-06	2.563603E-05	2.413254E-05
4.2	3.431828E-06	1.108400E-05	4.250244E-06	3.305885E-06	2.572520E-05	2.323898E-05
4.4	1.183374E-06	7.734691E-06	6.291670E-06	3.773403E-06	2.827109E-05	2.374609E-05
4.6	8.211583E-10	6.463074E-06	1.054908E-05	1.691971E-07	3.150279E-05	2.328291E-05
4.8	5.211668E-08	1.269629E-05	1.234634E-05	1.290442E-06	3.191597E-05	2.774457E-05
5	4.988638E-07	8.531558E-06	1.149756E-05	2.589611E-06	3.232288E-05	3.622375E-05

$$\begin{aligned}
\widehat{q}_{C-IV}(\tau) &= 0.4\left(2arc\tan^{-1}e^{(0.1\tau+2.7)}-\frac{\pi}{2}\right)-0.3\left(2arc\tan e^{(0.02\tau-0.7)}-\frac{\pi}{2}\right)+1.7\left(2arc\tan e^{(0.8\tau+1.1)}-\frac{\pi}{2}\right)\\
&+0.7\left(2arc\tan e^{(0.05\tau+1.7)}-\frac{\pi}{2}\right)-0.01\left(2arc\tan e^{(-0.02\tau+0.03)}-\frac{\pi}{2}\right)-0.5arc\tan e^{(-0.09\tau+0.1)}-\frac{\pi}{2}\Big)\\
&+0.4\left(2arc\tan e^{(-0.7\tau+0.1)}-\frac{\pi}{2}\right)+0.6\left(2arc\tan e^{(1.6\,\tau+0.4)}-\frac{\pi}{2}\right)-0.5\left(2arc\tan e^{(-0.9\tau-0.5)}-\frac{\pi}{2}\right)\\
&+1.6\left(2arc\tan e^{(-1.4\tau-0.5)}-\frac{\pi}{2}\right).
\end{aligned} \tag{28}$$

Table 5 represents the statistical analysis of the predator $p(\tau)$ and prey $q(\tau)$ for case IV. The values of the Min, Med, and SIR for solving the predator $p(\tau)$ and prey $q(\tau)$ indexes based on the NDPPM are tabulated in Table 5. These values have been calculated in interval 0 and 5. The Min, Med and SIR predator $p(\tau)$ for Case IV are 10^{-07} to 10^{-11}, 10^{-06} to 10^{-08} and 10^{-06} to 10^{-09}, while the Min, Med and SIR prey $q(\tau)$ values for Case IV are found around 10^{-06} to 10^{-10}, 10^{-06} to 10^{-08} and 10^{-05} to 10^{-08}. These negligible calculated values indicate the reliability of the stochastic solver.

Case V. Consider a NDPPM becomes by taking $a = 0.1, b = 0.014, c = 0.012, d = 0.03$, $\alpha_1 = 2$ and $\alpha_2 = 5$ values in Eq. (1) as:

$$\begin{cases} p'(\tau) = 0.1p(\tau) - 0.014p(\tau)q(\tau),\\ q'(\tau) = -0.012q(t) + 0.03p(\tau)q(t),\\ p(0) = 2, q(0) = 5. \end{cases} \tag{29}$$

A merit function for the above system (29) is written as:

$$\begin{aligned}\zeta_{Fit} = &\frac{1}{N}\sum_{i=1}^{N}\left(\left(\widehat{p}'_i - 0.1\widehat{p}_i + 0.014\widehat{p}_i\widehat{q}_i\right)^2 + \left(\widehat{q}'_i + 0.012q_i - 0.03\widehat{p}_i\widehat{q}_i\right)^2\right)\\ &+\frac{1}{2}\left(\left(\widehat{p}_0 - 2\right)^2 + \left(\widehat{q}_0 - 5\right)^2\right).\end{aligned} \tag{30}$$

The optimization performances using the GNNs-GA-IPA are performed to solve the case V that is obtained through GA-IPA for 20 independent trials to adjust the system parameters. The numerical results have been calculated in inputs 0 to 5 along with the 0.02 step size. The set of approximate results based $p(\tau)$ and $q(\tau)$ for case V are written as:

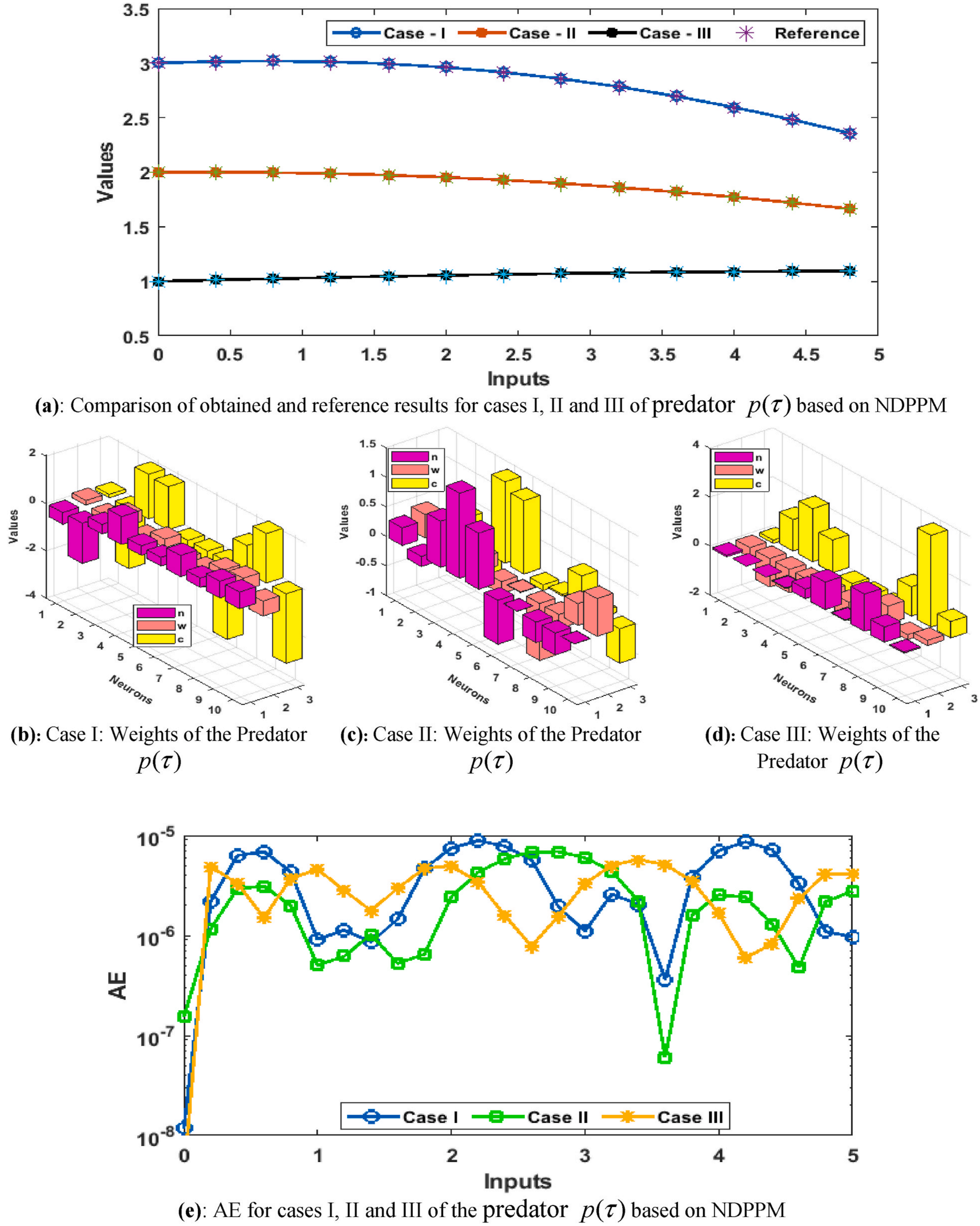

(**a**): Comparison of obtained and reference results for cases I, II and III of predator $p(\tau)$ based on NDPPM

(**b**): Case I: Weights of the Predator $p(\tau)$

(**c**): Case II: Weights of the Predator $p(\tau)$

(**d**): Case III: Weights of the Predator $p(\tau)$

(**e**): AE for cases I, II and III of the predator $p(\tau)$ based on NDPPM

Fig. 2. Best weight vectors of the GNNs-GA-IPA, results comparison and AE values for cases I, II and III of the predator $p(\tau)$ based on NDPPM **(a)**: Comparison of obtained and reference results for cases I, II and III of predator $p(\tau)$ based on NDPPM **(b)**: Case I: Weights of the Predator $p(\tau)$ **(c)**: Case II: Weights of the Predator $p(\tau)$ **(d)**: Case III: Weights of the Predator $p(\tau)$ **(e)**: AE for cases I, II and III of the predator $p(\tau)$ based on NDPPM.

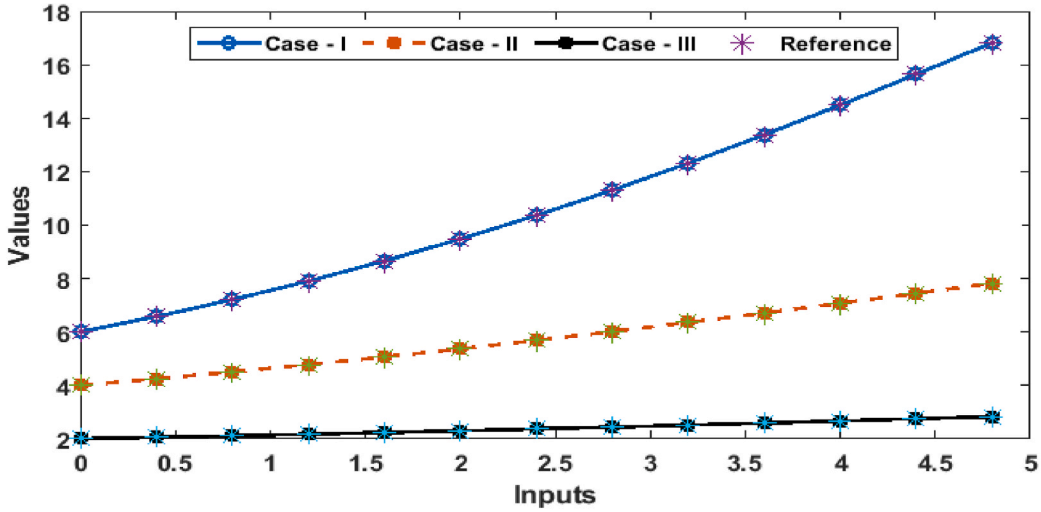

(a): Comparison of obtained and reference results for cases I, II and III for cases I, II and III of the prey $q(\tau)$ based on NDPPM

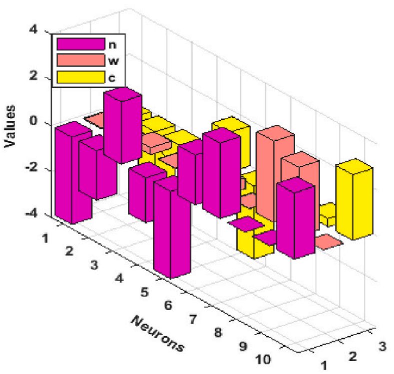

(b): Case I: Weights of the Prey $q(\tau)$

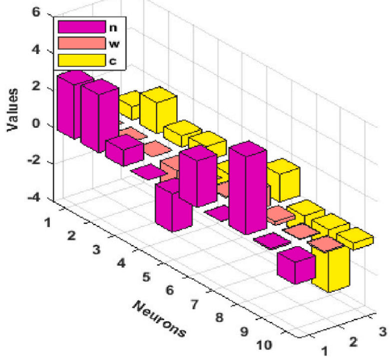

(c): Case II: Weights of the Prey $q(\tau)$

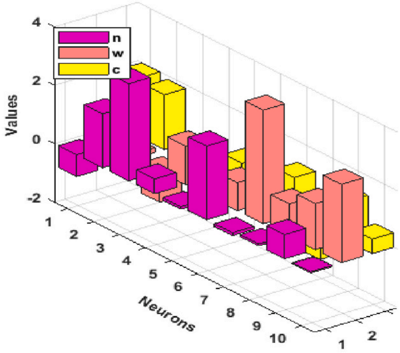

(d): Case III: Weights of the Prey $q(\tau)$

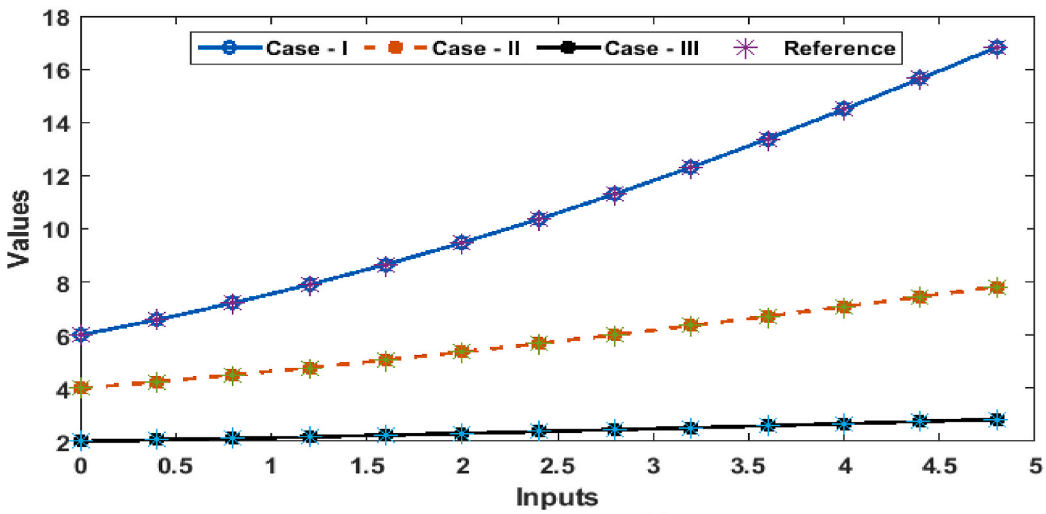

(e): AE for cases I, II and III of the Prey $q(\tau)$ based on NDPPM

Fig. 3. Best weight vectors of the GNNs-GA-IPA, results comparison and AE values for cases I, II and III of the Prey $q(\tau)$ based on NDPPM **(a)**: Comparison of obtained and reference results for cases I, II and III for cases I, II and III of the prey $q(\tau)$ based on NDPPM **(b)**: Case I: Weights of the Prey $q(\tau)$ **(c)**: Case II: Weights of the Prey $q(\tau)$ **(d)**: Case III: Weights of the Prey $q(\tau)$ **(e)**: AE for cases I, II and III of the Prey $q(\tau)$ based on NDPPM.

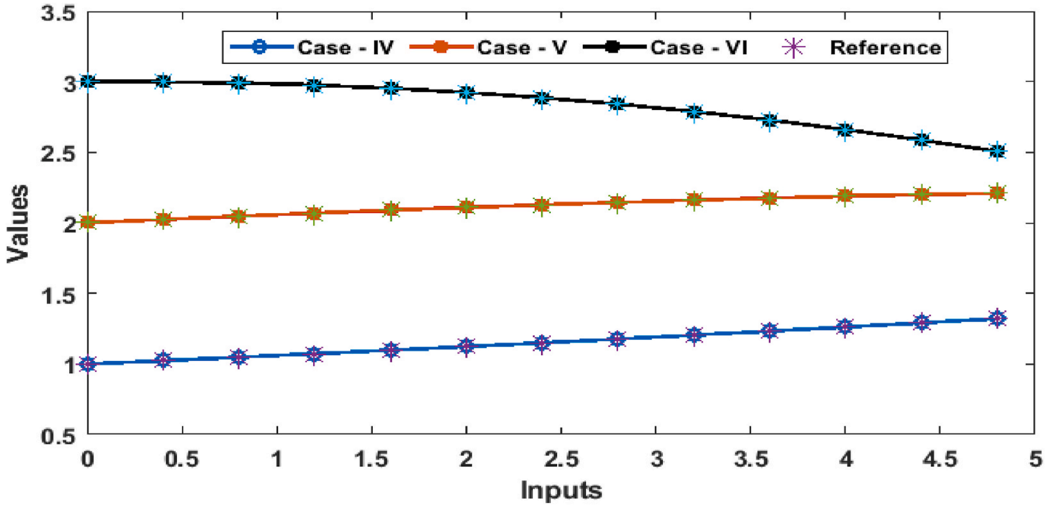

(a): Comparison of obtained and reference results for cases IV, V and VI of the predator $p(\tau)$ based on NDPPM

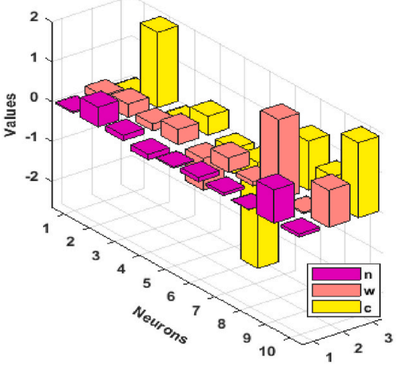

(b): Case I: Weights of the Predator $p(\tau)$

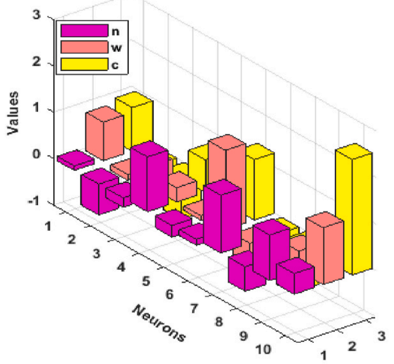

(c): Case II: Weights of the Predator $p(\tau)$

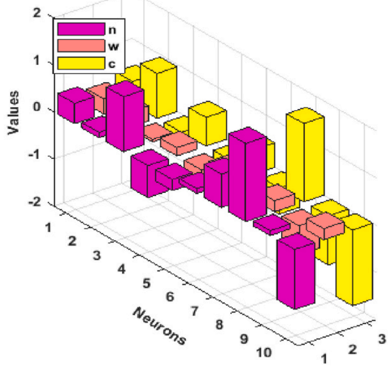

(d): Case III: Weights of the Predator $p(\tau)$

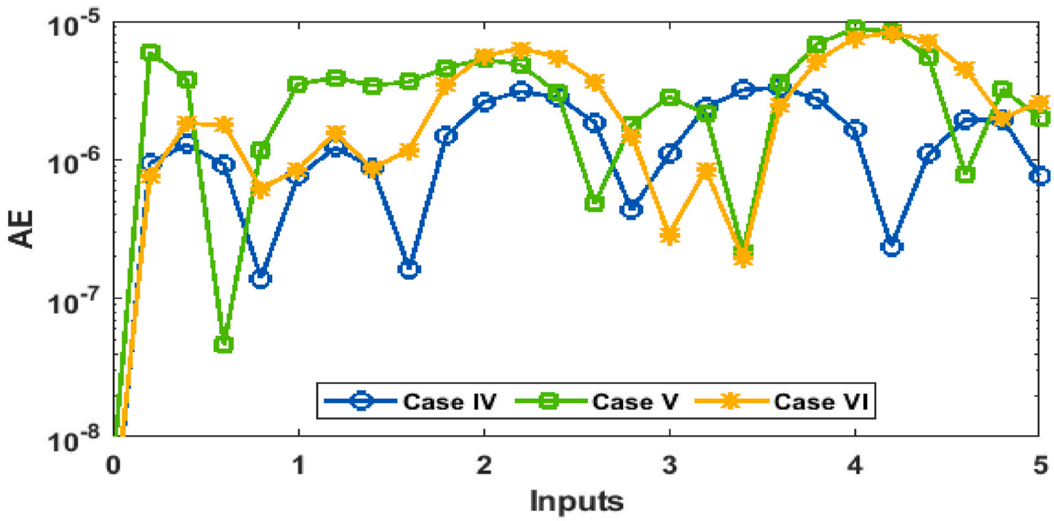

(e): AE for cases IV, V and VI of the predator $p(\tau)$ based on NDPPM

(caption on next page)

Fig. 4. Best weight vectors of the GNNs-GA-IPA, results comparison and AE values for cases IV, V and VI of the predator $p(\tau)$ based on NDPPM **(a):** Comparison of obtained and reference results for cases IV, V and VI of the predator $p(\tau)$ based on NDPPM **(b):** Case I: Weights of the Predator $p(\tau)$ **(c):** Case II: Weights of the Predator $p(\tau)$ **(d):** Case III: Weights of the Predator $p(\tau)$ **(e):** AE for cases IV, V and VI of the predator $p(\tau)$ based on NDPPM.

$$\begin{aligned}\widehat{p}_{C-V}(\tau)=&0.09\left(2arc\tan e^{(0.8\tau+0.9)}-\frac{\pi}{2}\right)-0.6\left(2arc\tan e^{(-0.1\tau-0.5)}-\frac{\pi}{2}\right)-0.2\left(2arc\tan e^{(0.4\tau-0.8)}-\frac{\pi}{2}\right)\\&+1.2\left(2arc\tan e^{(0.3\tau+0.7)}-\frac{\pi}{2}\right)-0.2\left(2arc\tan e^{(-0.09\tau+0.1)}-\frac{\pi}{2}\right)-0.1\left(2arc\tan e^{(1.7\tau+1.3)}-\frac{\pi}{2}\right)\\&+1.2\left(2arc\tan e^{(-0.5\tau-0.1)}-\frac{\pi}{2}\right)-0.5\left(2arc\tan e^{(0.1\tau-0.8)}-\frac{\pi}{2}\right)+0.9\left(2arc\tan e^{(0.4\tau-0.04)}-\frac{\pi}{2}\right)\\&+0.4\left(2arc\tan e^{(1.2\tau+2.4)}-\frac{\pi}{2}\right),\end{aligned}\tag{31}$$

$$\begin{aligned}\widehat{q}_{C-V}(\tau)=&-1.7\left(2arc\tan e^{(7.9\tau-0.3)}-\frac{\pi}{2}\right)+2.6\left(2arc\tan e^{(-0.1\tau-1.6)}-\frac{\pi}{2}\right)+2.7\left(2arc\tan e^{(-0.005\tau+1.6)}-\frac{\pi}{2}\right)\\&-2.0\left(2arc\tan e^{(-0.009\tau-0.2)}-\frac{\pi}{2}\right)+1.3\left(2arc\tan e^{(0.08\tau+0.09)}-\frac{\pi}{2}\right)-1.8\left(2arc\tan e^{(0.006\tau-2.8)}-\frac{\pi}{2}\right)\\&-0.8\left(2arc\tan e^{(-0.02\tau-0.5)}-\frac{\pi}{2}\right)-0.3\left(2arc\tan e^{(-0.13\tau+0.4)}-\frac{\pi}{2}\right)-1.6\left(2arc\tan e^{(0.01\tau-0.4)}-\frac{\pi}{2}\right)\\&+1.5\left(2arc\tan e^{(-0.04\tau-0.05)}-\frac{\pi}{2}\right).\end{aligned}\tag{32}$$

Table 6 represents the statistical analysis of the predator $p(\tau)$ and prey $q(\tau)$ of case V based on the NDPPM. The values of the Min, Med, and SIR for solving the predator $p(\tau)$ and prey $q(\tau)$ indexes based on the NDPPM are tabulated in Table 6. These values have been calculated in the interval 0 and 5. The Min, Med and SIR predator $p(\tau)$ performances for case V are calculated as 10^{-06} to 10^{-09}, 10^{-05} to 10^{-07} and 10^{-06} to 10^{-07}, while the Min, Med and SIR prey $q(\tau)$ values for case V are found around 10^{-06} to 10^{-11}, 10^{-05} to 10^{-07} and 10^{-06} to 10^{-07}. These small results indicate the reliability and exactness of proposed method.

Case VI. Consider a NDPPM with $a = 0.1, b = 0.014, c = 0.012, d = 0.05$, $\alpha_1 = 3$ and $\alpha_2 = 7$. The NDPPM based system (1) is updated as:

$$\begin{cases}p'(\tau)=0.1p(\tau)-0.014p(\tau)q(\tau),\\q'(\tau)=-0.012q(t)+0.05p(\tau)q(t),\\p(0)=3,q(0)=7.\end{cases}\tag{33}$$

A merit function for the above system (33) is written as:

$$\begin{aligned}\zeta_{Fit}=&\frac{1}{N}\sum_{i=1}^{N}\left((\widehat{p}'_i-0.1\widehat{p}_i+0.014\widehat{p}_i\widehat{q}_i)^2+(\widehat{q}'_i+0.012q_i-0.05\widehat{p}_i\widehat{q}_i)^2\right)\\&+\frac{1}{2}\left((\widehat{p}_0-3)^2+(\widehat{q}_0-7)^2\right).\end{aligned}\tag{34}$$

The optimization performances using the GNNs-GA-IPA to solve the case VI based on the NDPPM is obtained through the hybrid of GA-IPA for 20 independent trials. The numerical results have been calculated in inputs 0 to 5 along with the 0.02 step size. The set of approximate results of $p(\tau)$ and $q(\tau)$ for case VI are written as:

$$\begin{aligned}\widehat{p}_{C-VI}(\tau)=&0.4\left(2arc\tan e^{(0.3\tau+0.4)}-\frac{\pi}{2}\right)+0.1\left(2arc\tan e^{(0.3\tau+0.9)}-\frac{\pi}{2}\right)+1.1\left(2arc\tan e^{(0.05\tau-0.1)}-\frac{\pi}{2}\right)-0.6\left(2arc\tan e^{(0.1\tau+0.6)}-\frac{\pi}{2}\right)\\&-0.2\left(2arc\tan e^{(-0.2\tau+0.8)}-\frac{\pi}{2}\right)-0.1\left(2arc\tan e^{(0.2\tau+0.5)}-\frac{\pi}{2}\right)\\&+0.7\left(2arc\tan e^{(-0.2\tau-1.6)}-\frac{\pi}{2}\right)+1.6\left(2arc\tan e^{(0.2\tau+1.6)}-\frac{\pi}{2}\right)+0.1\left(2arc\tan e^{(-0.6\tau-1)}-\frac{\pi}{2}\right)-1.2\left(2arc\tan e^{(0.2\tau-1.6)}-\frac{\pi}{2}\right),\end{aligned}\tag{35}$$

$$\begin{aligned}\widehat{q}_{C-VI}(\tau)=&-0.4\left(2arc\tan e^{(-2.0\tau-2.2)}-\frac{\pi}{2}\right)-2\left(2arc\tan e^{(-0.02\tau-0.3)}-\frac{\pi}{2}\right)-2.4\left(2arc\tan e^{(-0.3\tau+2.0)}-\frac{\pi}{2}\right)\\&+0.2\left(2arc\tan e^{(1.6\tau+1.6)}-\frac{\pi}{2}\right)+0.7\left(2arc\tan e^{(-1.8\tau-2.08)}-\frac{\pi}{2}\right)-2.7\left(2arc\tan e^{(-0.1\tau-1.3)}-\frac{\pi}{2}\right)-2.9\left(2arc\tan e^{(-0.2\tau+0.8)}-\frac{\pi}{2}\right)\\&+0.2\left(2arc\tan e^{(-0.9\tau-2.2)}-\frac{\pi}{2}\right)-2.2\left(2arc\tan e^{(-0.07\tau-1.9)}-\frac{\pi}{2}\right)\\&+4.2\left(2arc\tan e^{(0.07\tau+2.9)}-\frac{\pi}{2}\right).\end{aligned}\tag{36}$$

Table 7 provides the statistical analysis of the predator $p(\tau)$ and prey $q(\tau)$ of case VI based on the NDPPM. The values of the Min, Med, and SIR for solving the predator $p(\tau)$ and prey $q(\tau)$ indexes based on the NDPPM are tabulated in Table 7. These values have been calculated in interval 0 and 5. The Min, Med and SIR predator $p(\tau)$ representations for Case VI are shown as 10^{-06} to 10^{-10}, 10^{-05} to

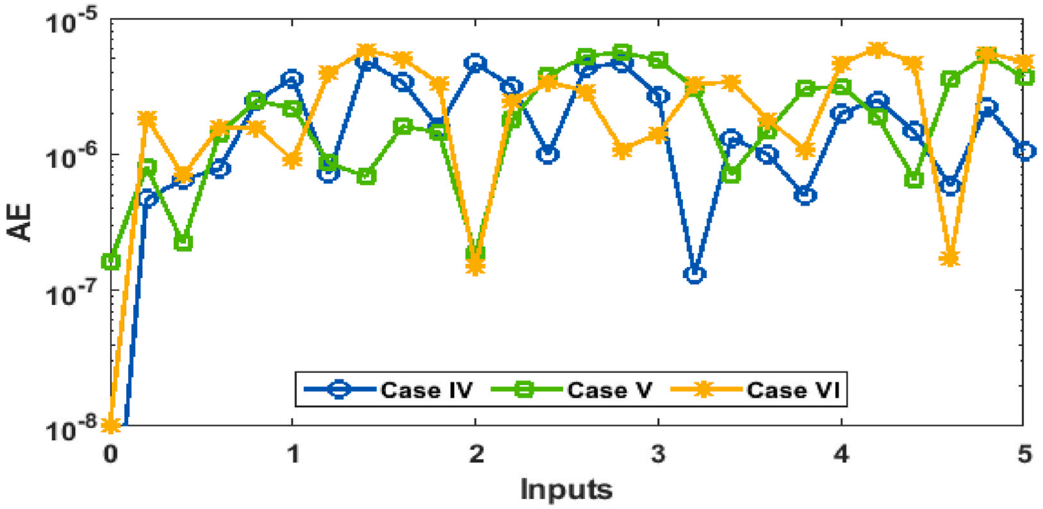

(a): Comparison of obtained and reference results for cases IV, V and VI of the Prey $q(\tau)$ based on NDPPM

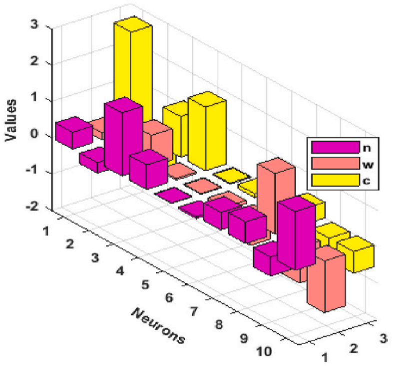

(b): Case I: Weights of the Prey $q(\tau)$

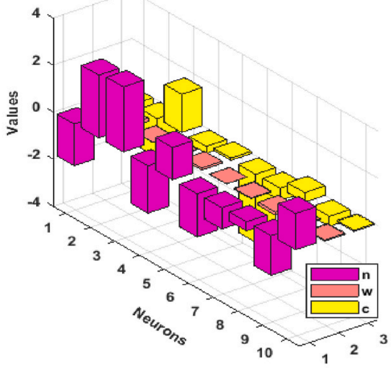

(c): Case II: Weights of the Prey $q(\tau)$

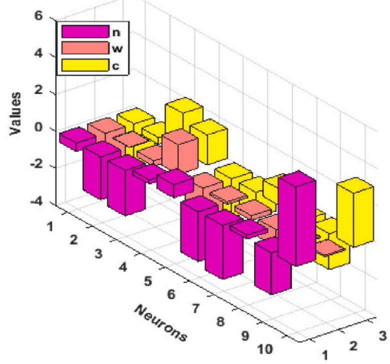

(d): Case III: Weights of the Prey $q(\tau)$

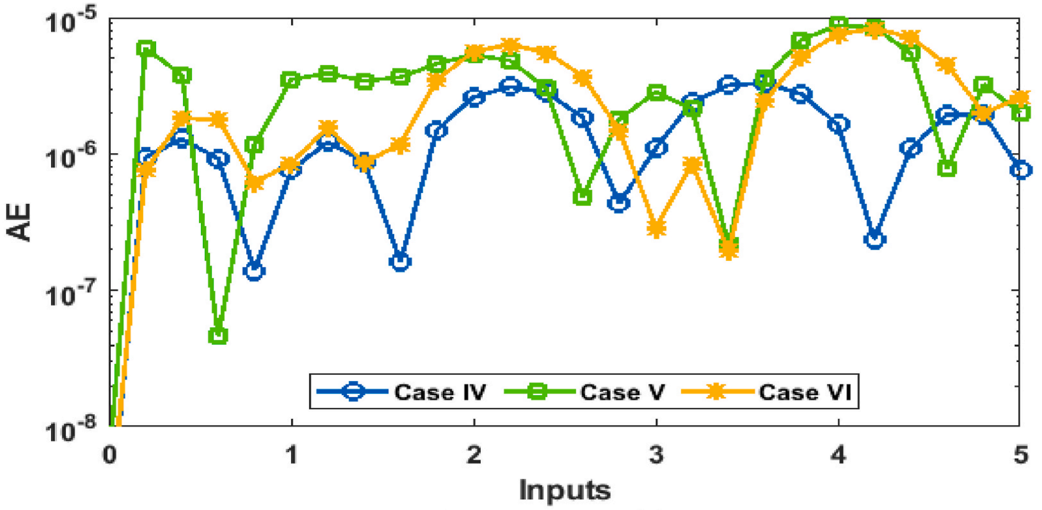

(e): AE for cases IV, V and VI of the Prey $q(\tau)$ based on NDPPM

Fig. 5. Best weight vectors of the GNNs-GA-IPA, results comparison and AE values for cases IV, V and VI of the Prey $q(\tau)$ based on NDPPM **(a)**: Comparison of obtained and reference results for cases IV, V and VI of the Prey $q(\tau)$ based on NDPPM **(b):** Case I: Weights of the Prey $q(\tau)$ **(c):** Case II: Weights of the Prey $q(\tau)$ **(d):** Case III: Weights of the Prey $q(\tau)$ **(e):** AE for cases IV, V and VI of the Prey $q(\tau)$ based on NDPPM.

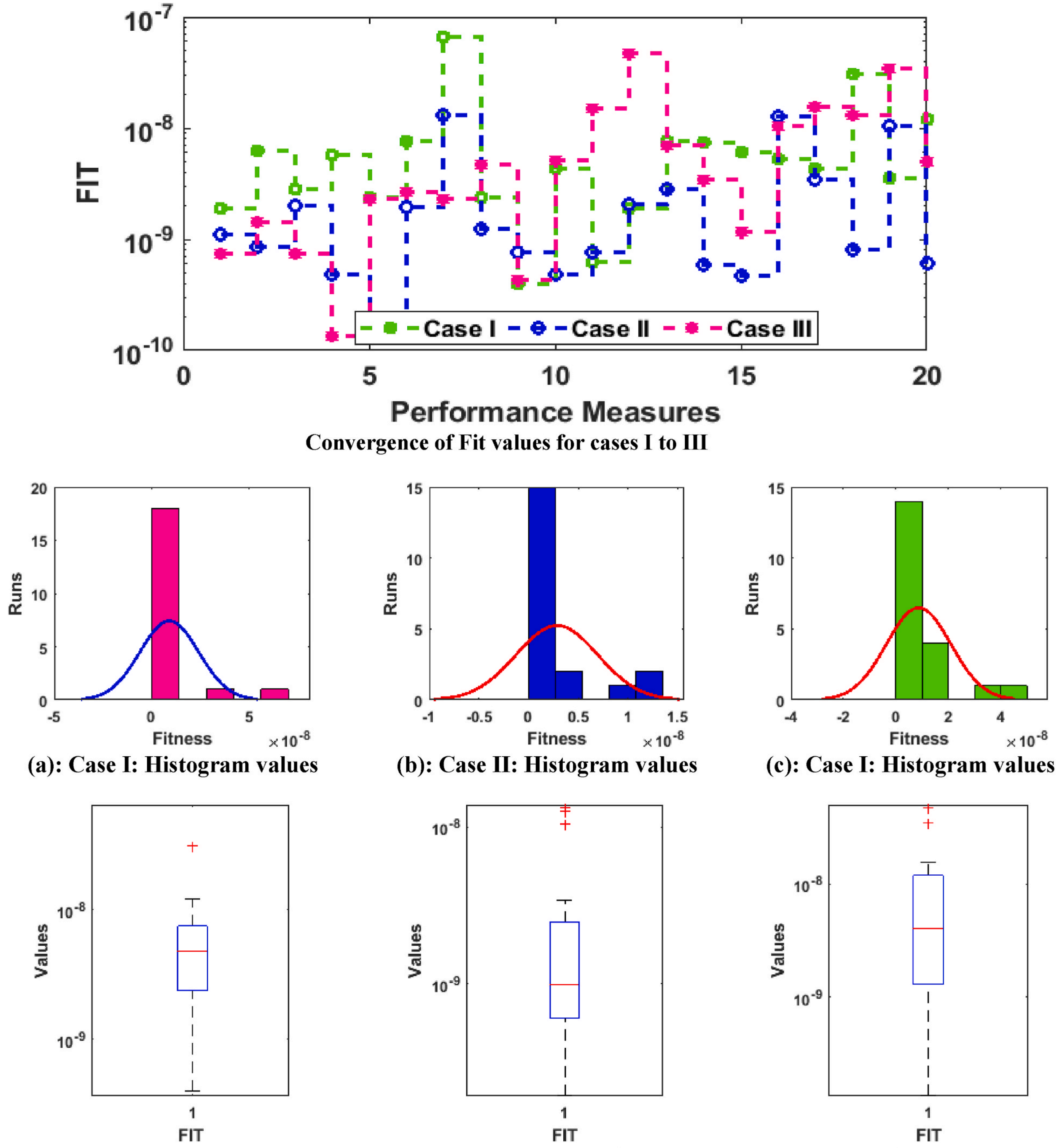

Convergence of Fit values for cases I to III

(a): Case I: Histogram values (b): Case II: Histogram values (c): Case I: Histogram values

(a): Case I: Boxplots (b): Case II: Boxplots (c): Case III: Boxplots

Fig. 6. Fitness, Histograms and Boxplots for Cases 1, II and III based on NDPPM Convergence of Fit values for cases I to III (a): Case I: Histogram values (b): Case II: Histogram values (c): Case I: Histogram values (a): Case I: Boxplots (b): Case II: Boxplots (c): Case III: Boxplots.

10^{-07} and 10^{-06} to 10^{-07}, while the Min, Med and SIR prey $q(\tau)$ values for Case VI are found around 10^{-06} to 10^{-09}, 10^{-05} to 10^{-08} and 10^{-05} to 10^{-07}. The small values reveal the reliability and exactness of proposed GNNs-GA-IPA.

Figs. 2–5 represent the best weight vectors of the GNNs-GA-IPA, results comparison, and AE values for each case of the predator $p(\tau)$ and prey $q(\tau)$ based on NDPPM. The weight vector values for the predator $p(\tau)$ are drawn in Figs. 2 and 3 using Eqs (((15), (19), (23), (27), (31) and (35) for cases I to VI. While the weight vector values for the prey $q(\tau)$ are drawn in Figs. 4 and 5 using Eqs (((16), (20), (24), (28), (32) and (35) for case I, II, III, IV, V and VI. The comparison of the results is provided in Figs. 2–5 for each case of the predator $p(\tau)$ and prey $q(\tau)$ based on NDPPM. The results using the designed solver are matched with reference outcomes for each case

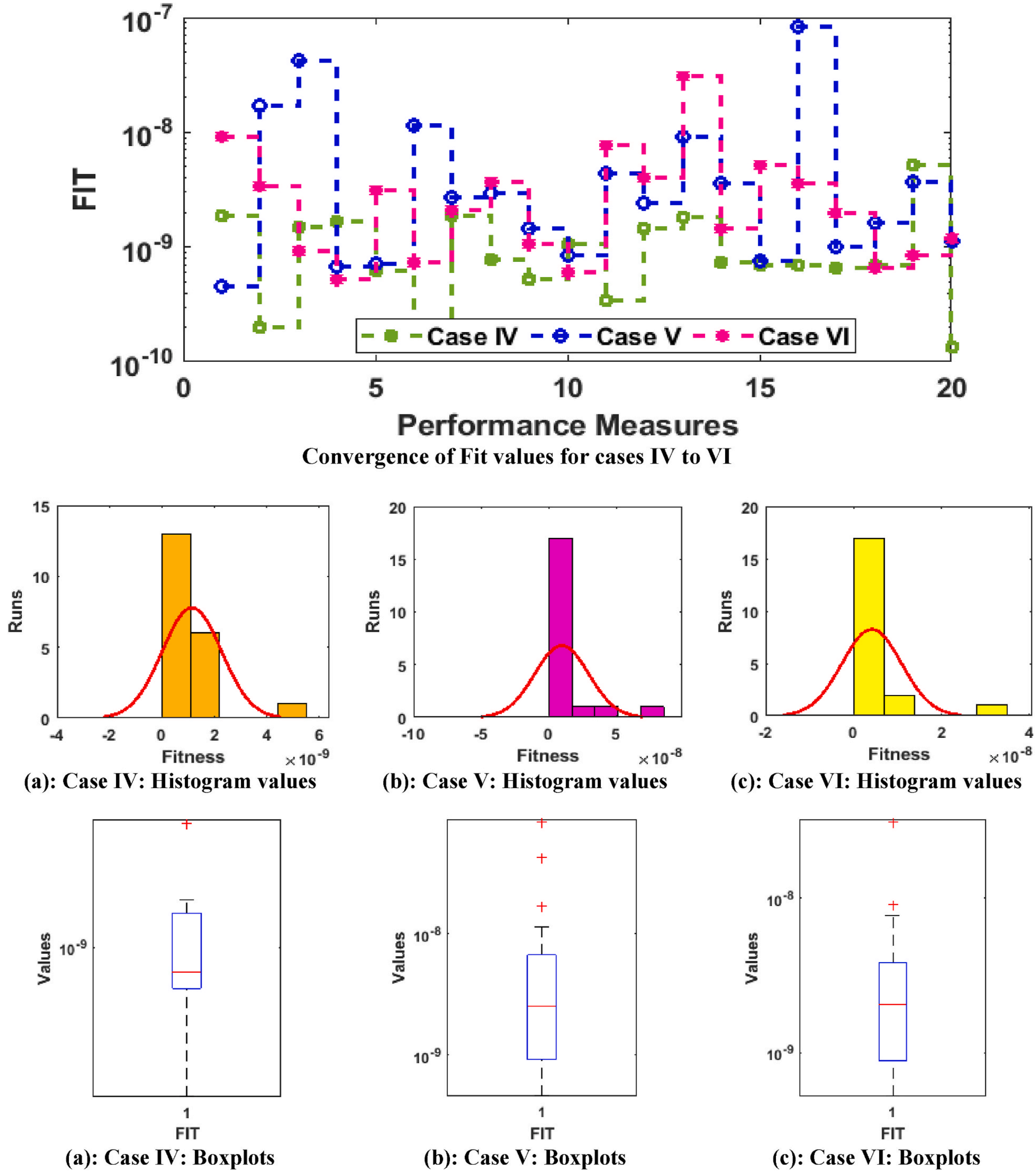

Fig. 7. Fitness, Histograms and Boxplots for Cases IV, V and VI based on NDPPM Convergence of Fit values for cases IV to VI (a): Case IV: Histogram values (b): Case V: Histogram values (c): Case VI: Histogram values (a): Case IV: Boxplots (b): Case V: Boxplots (c): Case VI: Boxplots.

of $p(\tau)$ and $q(\tau)$ based on NDPPM. These overlapping indicates the correctness and exactness of the designed GNNs-GA-IPA.

For the comparisons of the outcomes, the AE results are plotted in Figs. 2–5 for both indexes predator $p(\tau)$ and prey $q(\tau)$ based on NDPPM. For the index $p(\tau)$, the AE values for case I to VI are plotted in Figs. 2 and 3, while for the index $q(\tau)$, the AE are plotted in Figs. 4 and 5. One can observe that the AE for cases I and III of the predator category is found around 10^{-05} to 10^{-06}, while for case II, the AE values are found around 10^{-05} to 10^{-07}. The AE for cases IV, V and VI of the predator categories found as 10^{-06} - 10^{-07}, 10^{-05} - 10^{-07} and 10^{-05} - 10^{-06}. The AE for cases I to III of prey categories found as 10^{-05} to 10^{-07}, 10^{-06} to 10^{-08} and 10^{-05} to 10^{-06}. While

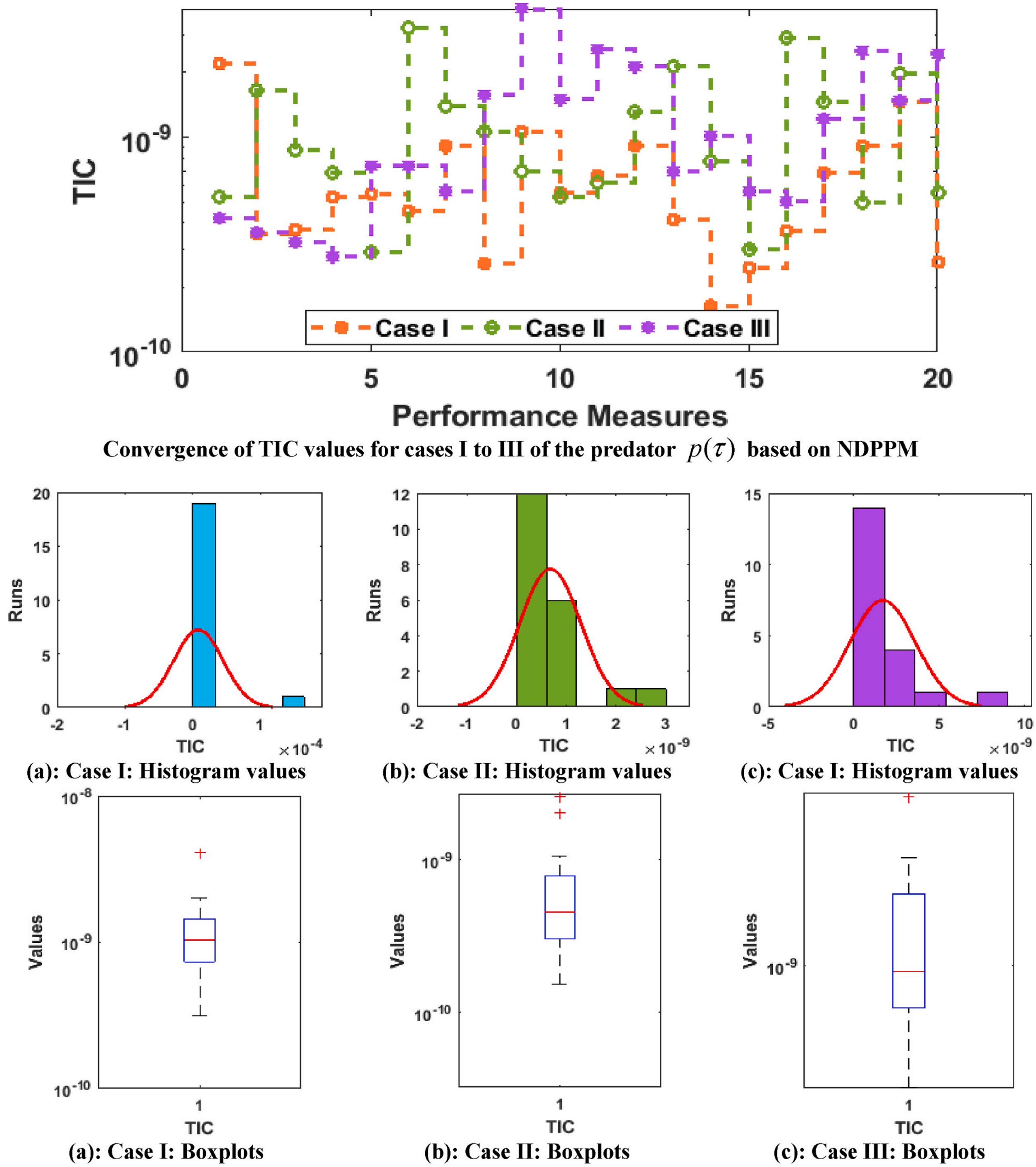

Fig. 8. TIC, Histograms and Boxplots for Cases 1, II and III of the predator $p(\tau)$ based on NDPPM Convergence of TIC values for cases I to III of the predator $p(\tau)$ based on NDPPM (a): Case I: Histogram values (b): Case II: Histogram values (c): Case I: Histogram values (a): Case I: Boxplots (b): Case II: Boxplots (c): Case III: Boxplots.

the AE for case IV is found as 10^{-05} to 10^{-07} and for cases V and VI, the predator categories found around 10^{-06} to 10^{-07}. These obtained numerical outcomes authenticate the competence of the solver.

Figs. 6 and 7 represent the Fitness (Fit), Histograms and Boxplots performances for Cases I-VI based on the NDPPM. Fig. 6 shows the Fit for Cases I to III, which lie as 10^{-07} - 10^{-09}, 10^{-07} - 10^{-10} and 10^{-08} - 10^{-10}, respectively. The Fit for Cases IV, V and VI are drawn in Fig. 7, which lie around 10^{-08} to 10^{-10}, 10^{-08} to 10^{-09} and 10^{-07} to 10^{-09}, respectively. These observations designate the exactness,

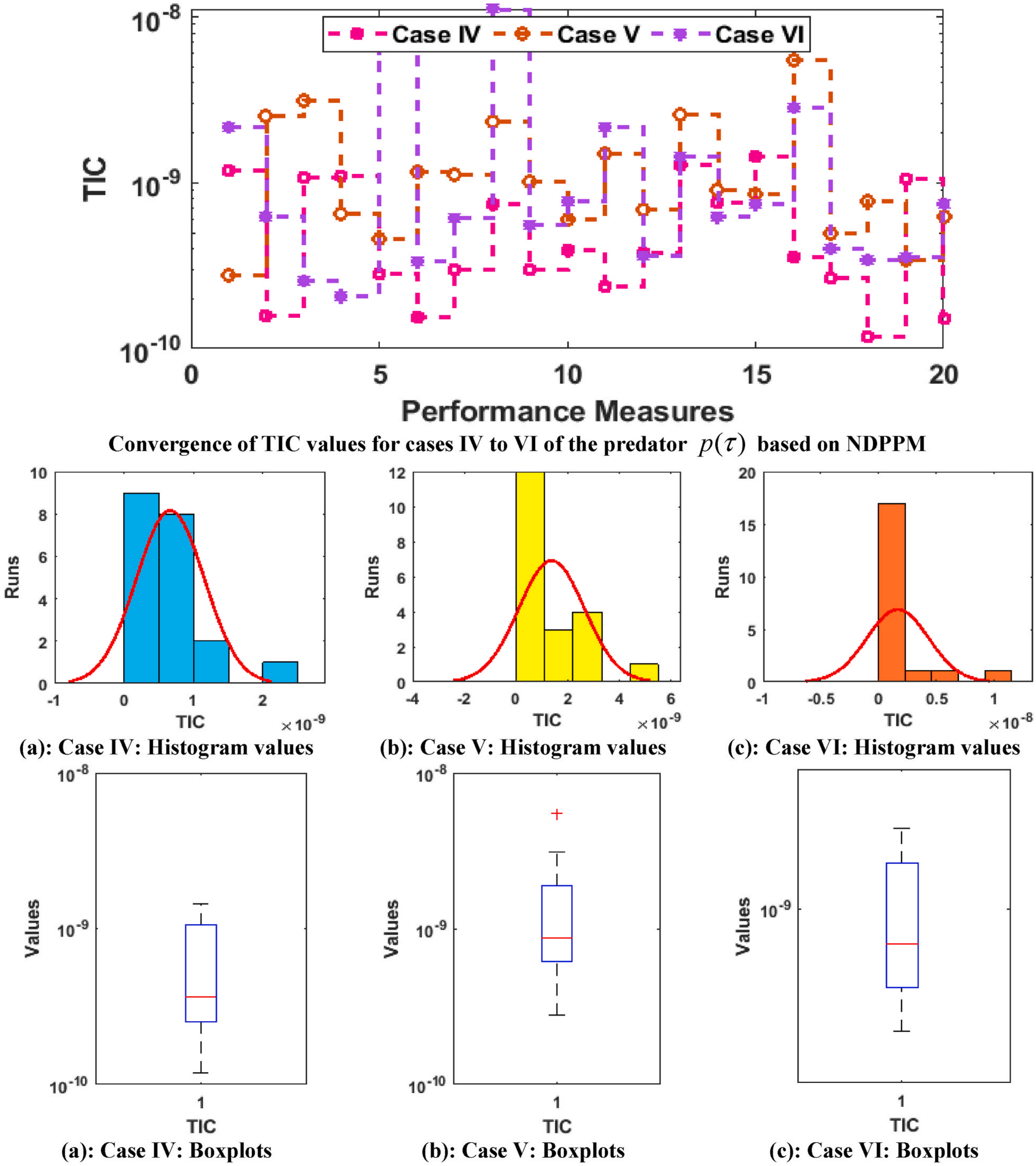

Fig. 9. TIC, Histograms and Boxplots for Cases IV, V and VI of the predator $p(\tau)$ based on NDPPM Convergence of TIC values for cases IV to VI of the predator $p(\tau)$ based on NDPPM (a): Case IV: Histogram values (b): Case V: Histogram values (c): Case VI: Histogram values (a): Case IV: Boxplots (b): Case V: Boxplots (c): Case VI: Boxplots.

and reliability of the scheme.

Figs. 8–11 indicates the performance of TIC, Histograms and Boxplots for Cases I-VI based on the NDPPM. It is observed in Fig. 8 that TIC values for the category $p(\tau)$ for Cases I to III lie as 10^{-09} to 10^{-10} and the TIC values for Cases IV, V and VI found as 10^{-09} - 10^{-10}, 10^{-08} - 10^{-10} and 10^{-08} - 10^{-09}. These TIC measures for the category $q(\tau)$ for Cases I to III are shown as 10^{-09} - 10^{-10}, 10^{-08} - 10^{-09} and 10^{-08} - 10^{-10}, respectively. The performances of TIC based on the category $q(\tau)$ for Cases IV, V and VI are shown as 10^{-09} -

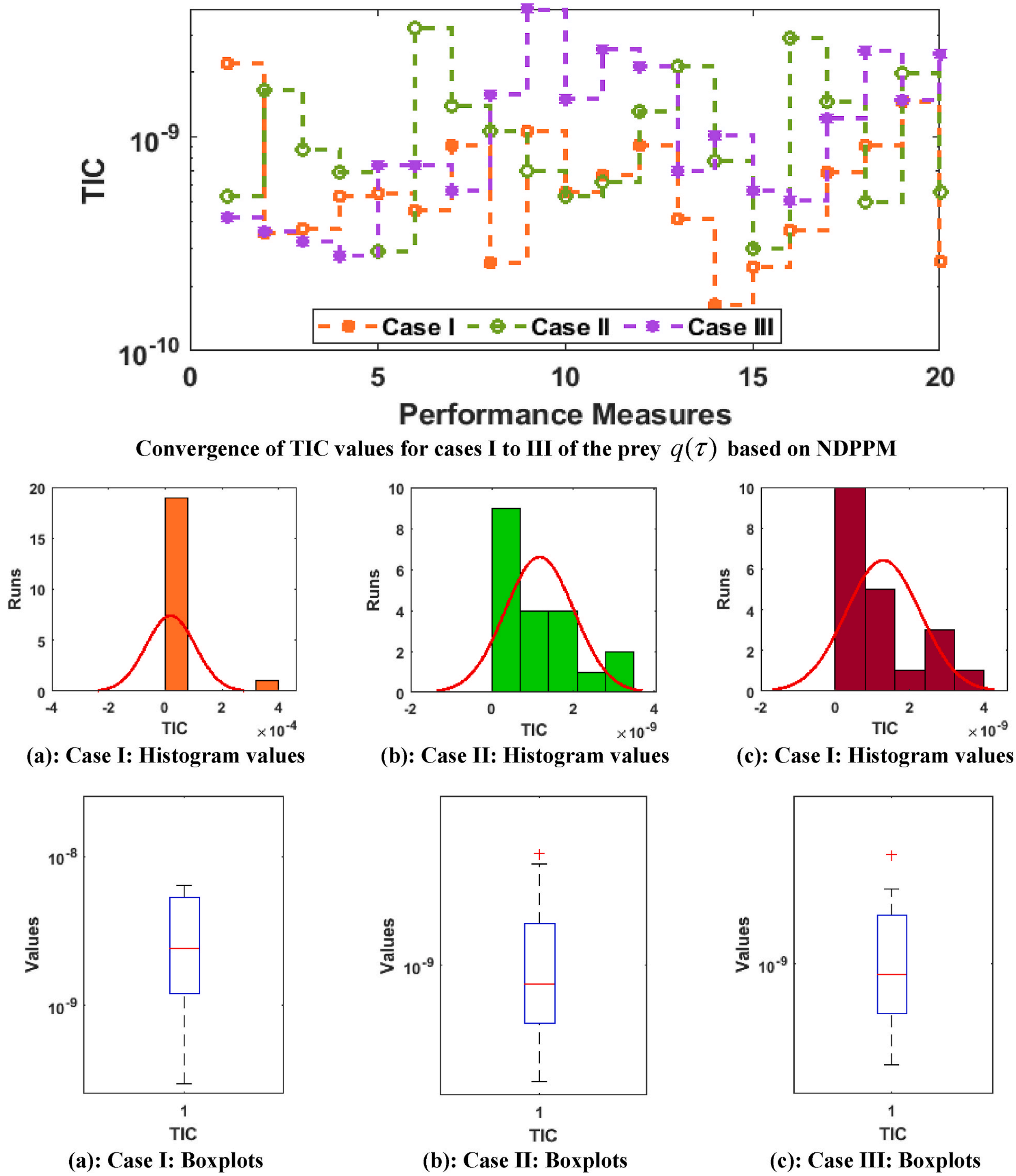

Fig. 10. TIC, Histograms and Boxplots for Cases 1, II and III of the prey $q(\tau)$ based on NDPPM Convergence of TIC values for cases I to III of the prey $q(\tau)$ based on NDPPM (a): Case I: Histogram values (b): Case II: Histogram values (c): Case I: Histogram values (a): Case I: Boxplots (b): Case II: Boxplots (c): Case III: Boxplots.

10^{-10}, 10^{-08} - 10^{-09} and 10^{-08} - 10^{-10}

Figs. 12–15 represent the performance of ENSE, Histograms and Boxplots for Cases I-VI. Fig. 12 shows that ENSE values for $p(\tau)$ lie as 10^{-08} - 10^{-10}, 10^{-10} - 10^{-12} and 10^{-07} - 10^{-10} for case I to III and ENSE for Cases IV, V and VI are shown as 10^{-08} - 10^{-11}, 10^{-09} - 10^{-11} and 10^{-10} - 10^{-12}. The values of ENSE for the category $q(\tau)$ for Cases I to III lie as 10^{-10} - 10^{-11}, 10^{-10} - 10^{-12} and 10^{-09} - 10^{-11},

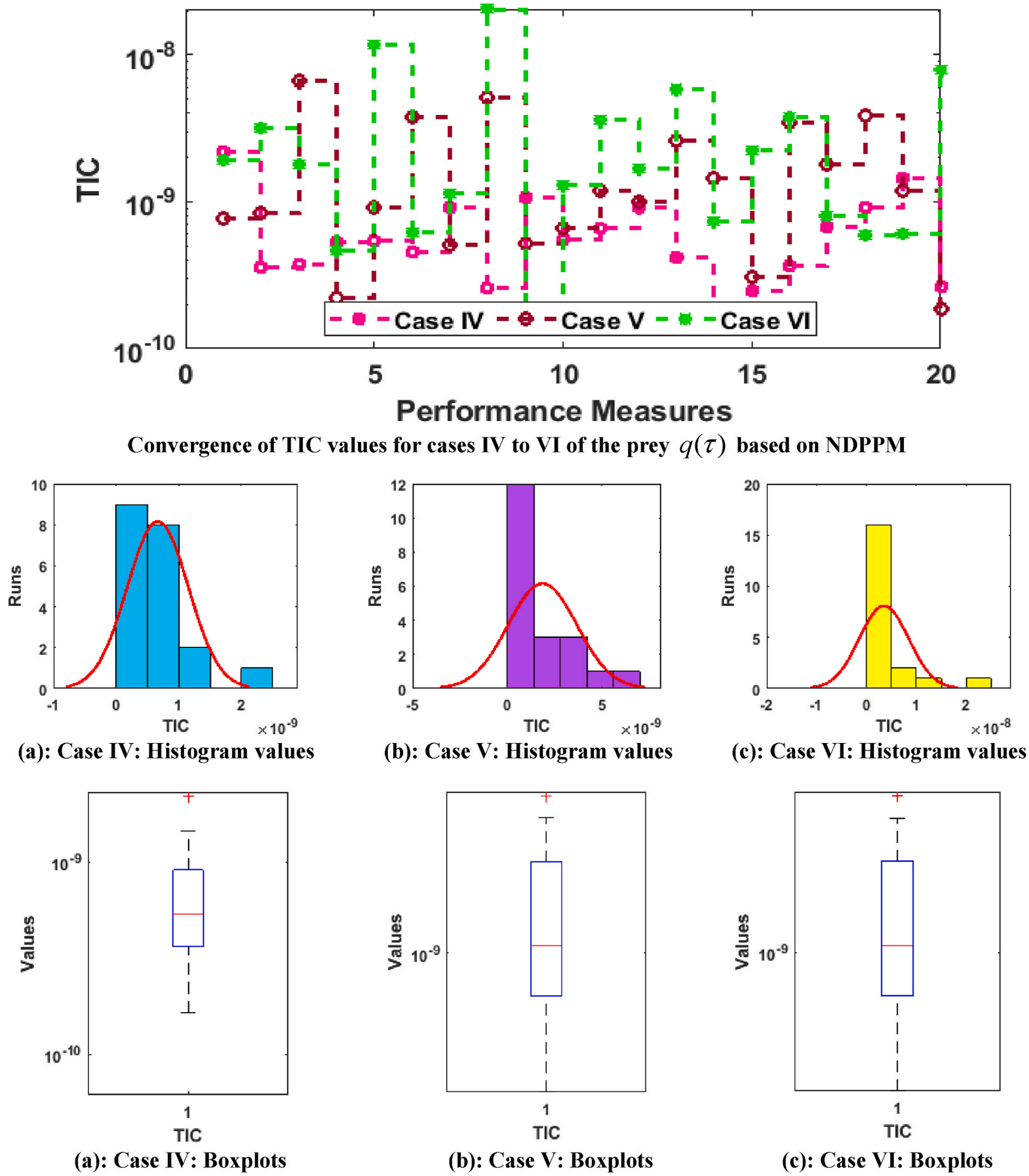

Fig. 11. TIC, Histograms and Boxplots for Cases IV, V and VI of the prey $q(\tau)$ based on NDPPM. Convergence of TIC values for cases IV to VI of the prey $q(\tau)$ based on NDPPM (a): Case IV: Histogram values (b): Case V: Histogram values (c): Case VI: Histogram values (a): Case IV: Boxplots (b): Case V: Boxplots (c):Case VI: Boxplots.

respectively. The TIC based category $q(\tau)$ for Cases IV, V and VI are shown as 10^{-11} - 10^{-12}, 10^{-10} - 10^{-12} and 10^{-09} - 10^{-12}. These observations represent the exactness, and reliability of the solver.

The comparison of the literature results and proposed solutions based on the designed stochastic procedures is presented in Table 8 for case 1 to 3 of predator class, while the comparison of pray class is tabulated in Table 9 for case 4 to 6. Similarly, the literature's

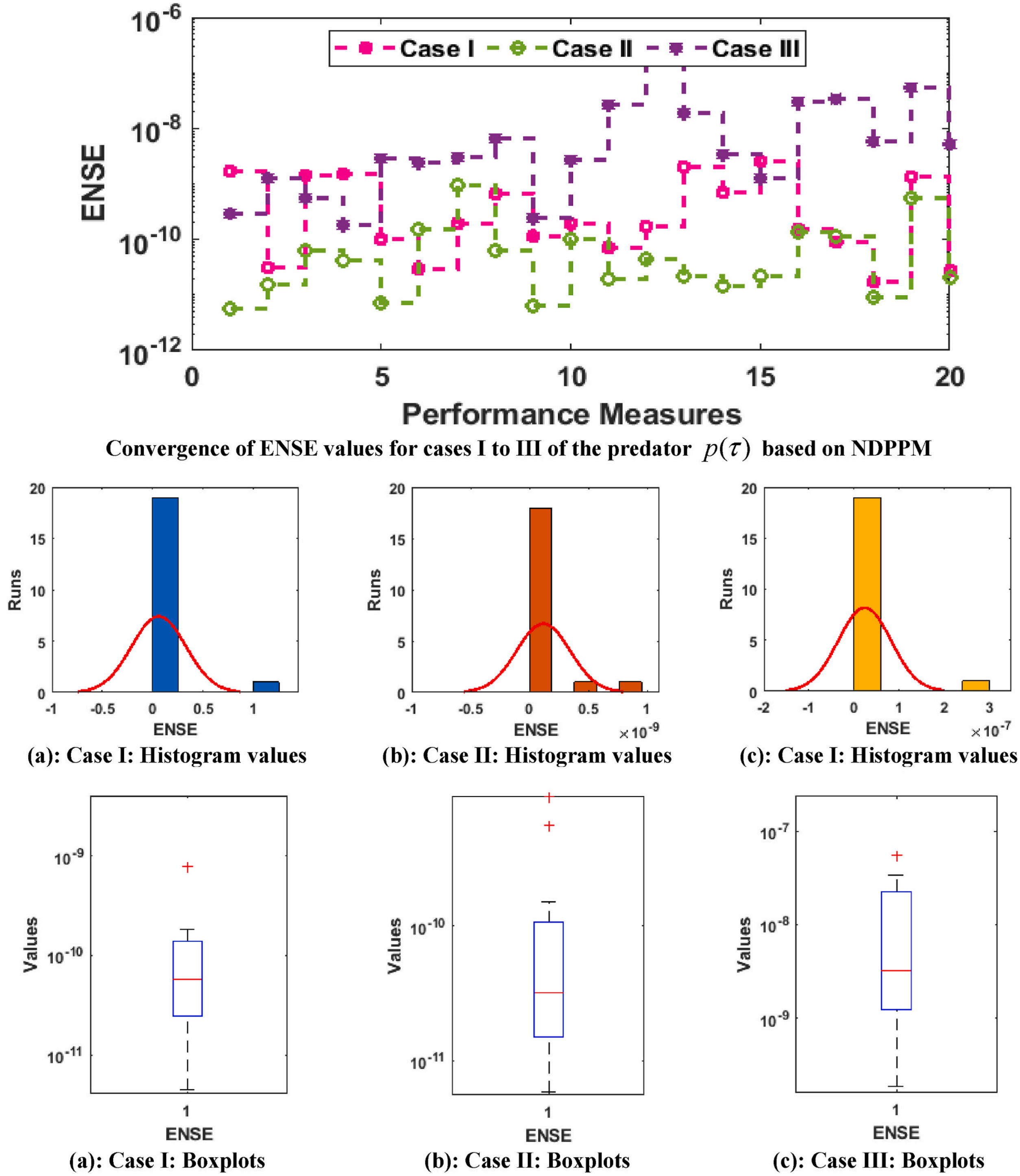

Fig. 12. ENSE, Histograms and Boxplots for Cases 1, II and III of the predator $p(\tau)$ based on NDPPM Convergence of ENSE values for cases I to III of the predator $p(\tau)$ based on NDPPM (a): Case I: Histogram values (b): Case II: Histogram values (c): Case I: Histogram values (a): Case I: Boxplots (b): Case II: Boxplots (c): Case III: Boxplots.

comparison is presented in Table 10 for case 1 to 3 of prey category, while the comparison of pray class is tabulated in Table 11 for case 4 to 6. Based on these tables, the Adams solution and the proposed results are overlapped to each other in good order. This shows the competence of the designed solver.

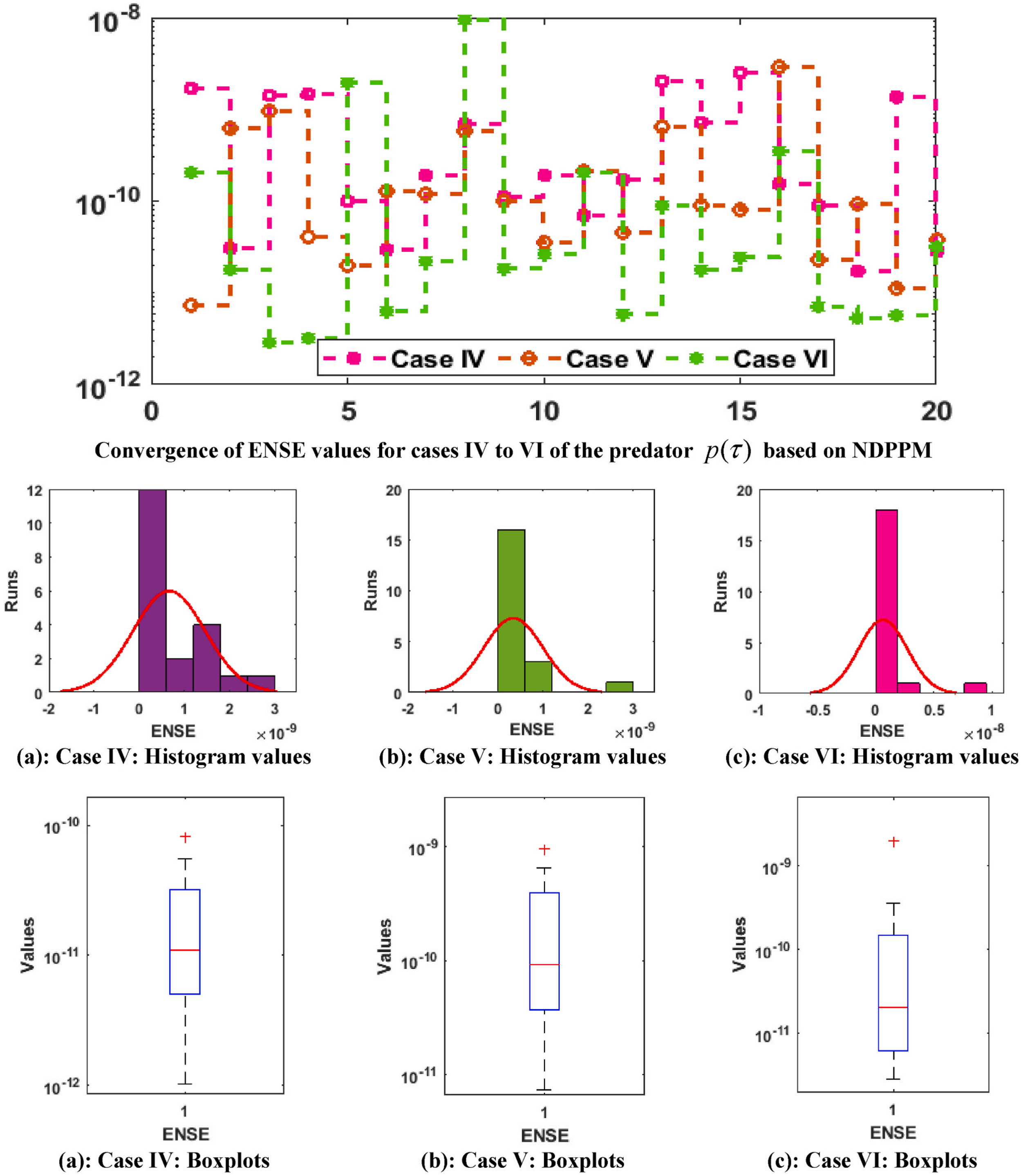

Fig. 13. ENSE, Histograms and Boxplots for Cases IV, V and VI of the predator $p(\tau)$ based on NDPPM Convergence of ENSE values for cases IV to VI of the predator $p(\tau)$ based on NDPPM (a): Case IV: Histogram values (b): Case V: Histogram values (c): Case VI: Histogram values (a):Case IV: Boxplots (b): Case V: Boxplots (c): Case VI: Boxplots.

4.1. Advantages of the GNNs over Runge-Kutta

ANNs and the conventional schemes like the Runge-Kutta (RK) serve a variety of purposes along with diverse advantages based on the problems. ANNs are extremely flexible systems, which are proficient to capture the nonlinear data association. ANNs can acquire

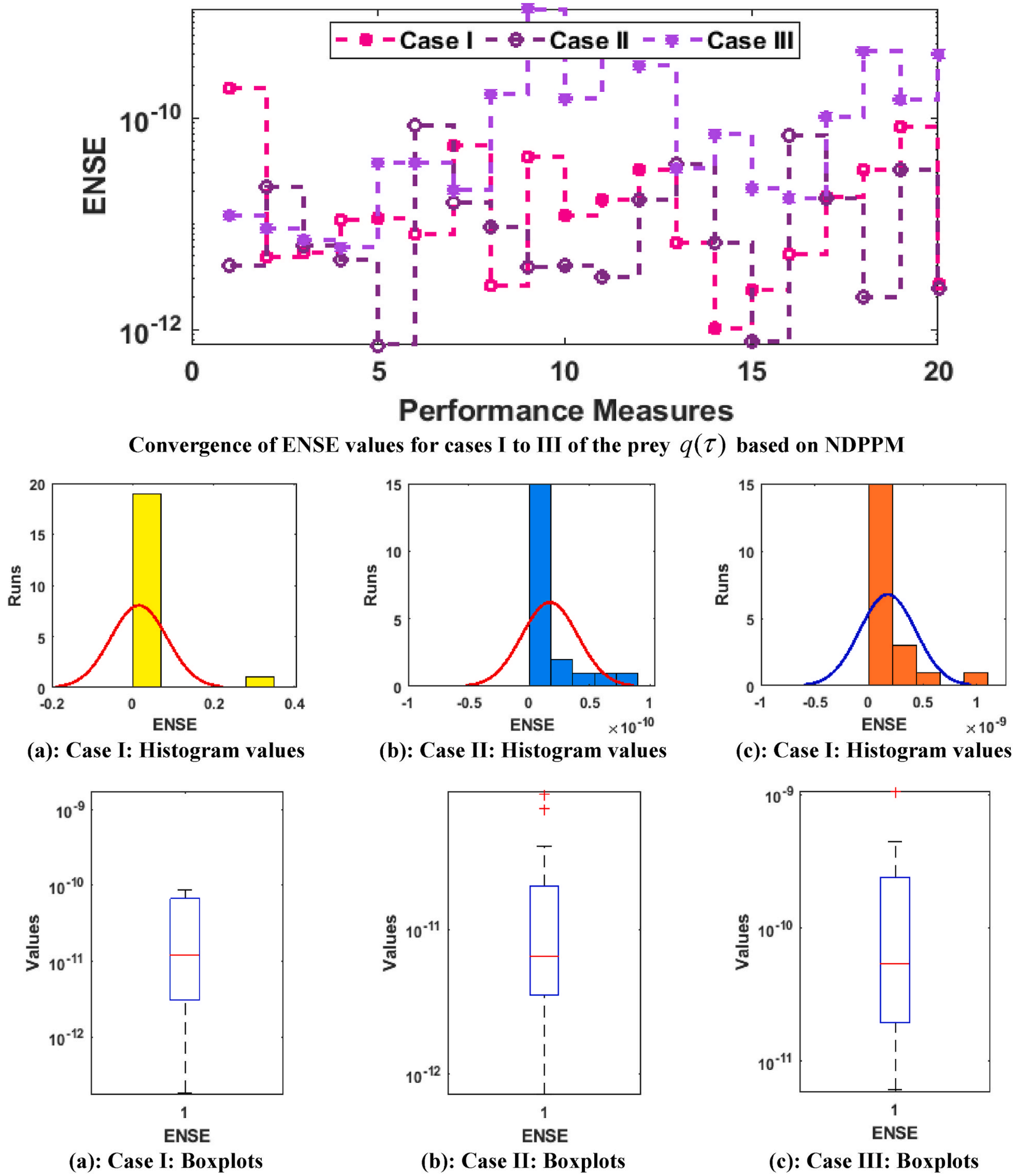

Fig. 14. ENSE, Histograms and Boxplots for Cases 1, II and III of the prey $q(\tau)$ based on NDPPM Convergence of ENSE values for cases I to III of the prey $q(\tau)$ based on NDPPM (a): Case I: Histogram values (b): Case II: Histogram values (c): Case I: Histogram values (a): Case I: Boxplots (b): Case II: Boxplots (c): Case III: Boxplots.

the complicated interactions that are not easy to handle by applying the deterministic schemes like RK. Another advantage of ANNs is to learn through the historical observations that is capable to predict or solve the problem using the data patterns. This competence of learning enables ANNs to deal with pattern recognition, classification, and regression that may not be directly agreeable by using the deterministic RK scheme. The stochastic computing solvers, such as GNNs characteristically describe the uncertainty, which is another

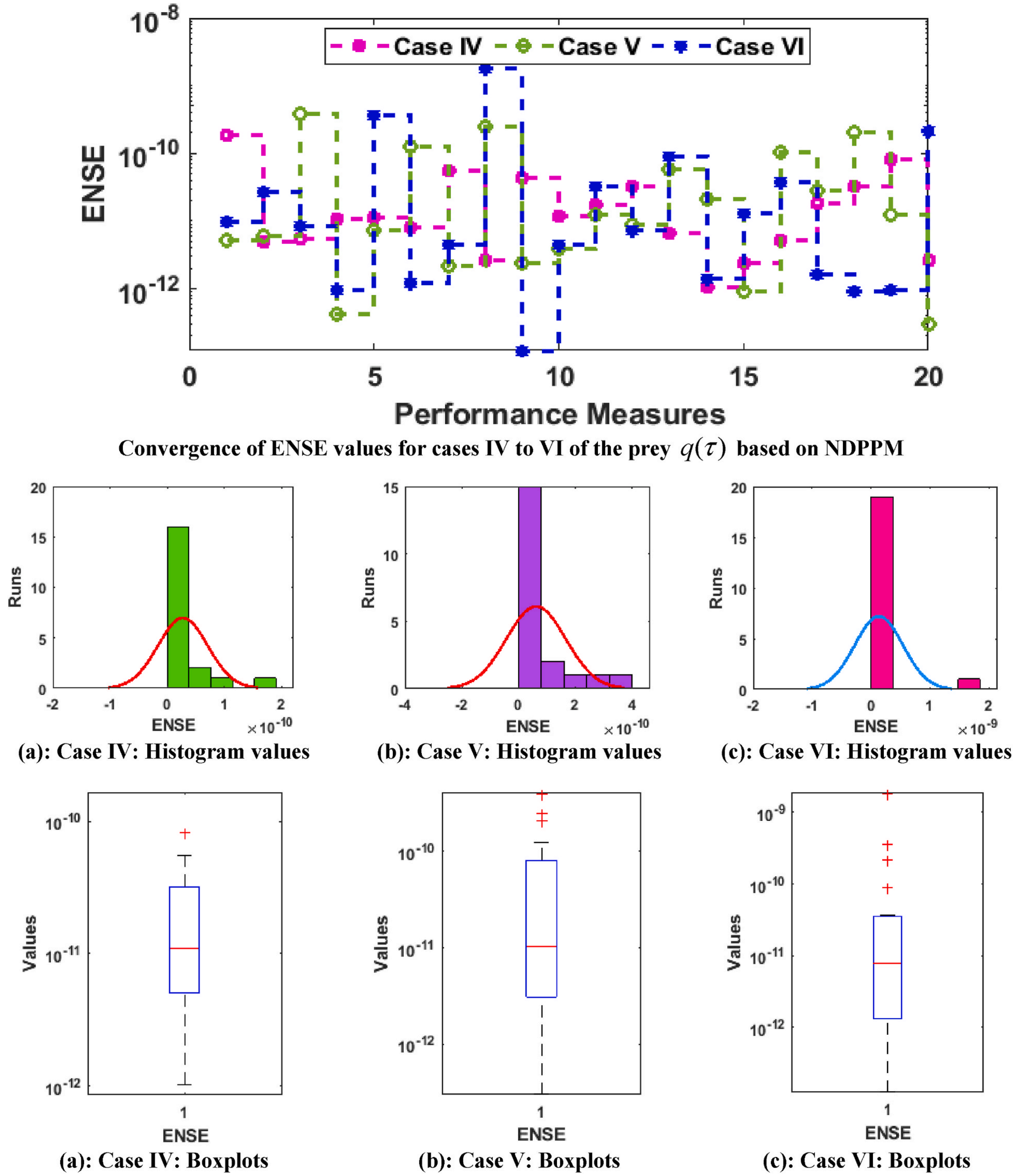

Fig. 15. ENSE, Histograms and Boxplots for Cases IV, V and VI of the prey $q(\tau)$ based on NDPPM Convergence of ENSE values for cases IV to VI of the prey $q(\tau)$ based on NDPPM (a): Case IV: Histogram values (b): Case V: Histogram values (c): Case VI: Histogram values (a): Case IV: Boxplots (b): Case V: Boxplots (c): Case VI: Boxplots.

advantage, where the fundamental dynamics are influenced through the arbitrary factors. ANNs present an adaptive system, which perform a nonlinear complicated data association. The ANNs based stochastic computing solvers can perform the scaled competently that permit to deal the problem with the large data along with the use of various parameters. This scalability performs in the numbers of applications in optimization, finance, and engineering.

Table 8
Comparison of the results for first three cases based on predator class $p(\tau)$.

τ	Proposed	Adams [55]	Proposed	Adams [55]	Proposed	Adams [55]
	Case 1	Case 1	Case 2	Case 2	Case 3	Case 3
	$p(\tau)$	$p(\tau)$	$p(\tau)$	$p(\tau)$	$p(\tau)$	$p(\tau)$
0	2.99999940	3.00000000	2.00000000	2.00000000	0.99999999	1.00000000
0.2	3.00844036	3.00844383	2.00102860	2.00102617	1.00632352	1.00632678
0.4	3.01447958	3.01448570	2.00088234	2.00088053	1.01249710	1.01250235
0.6	3.01798732	3.01799201	1.99952965	1.99952822	1.01851576	1.01851930
0.8	3.01882962	3.01883109	1.99693881	1.99693642	1.02436840	1.02437023
1	3.01687535	3.01687463	1.99307742	1.99307461	1.03004551	1.03004765
1.2	3.01199950	3.01199906	1.98791691	1.98791485	1.03554010	1.03554399
1.4	3.00408486	3.00408723	1.98143326	1.98143214	1.04084616	1.04085164
1.6	2.99302331	2.99303009	1.97360581	1.97360478	1.04595719	1.04596291
1.8	2.97871707	2.97872849	1.96441653	1.96441443	1.05086562	1.05087013
2	2.96108011	2.96109509	1.95385041	1.95384687	1.05556295	1.05556558
2.2	2.94003973	2.94005605	1.94189633	1.94189171	1.06004042	1.06004154
2.4	2.91553838	2.91555409	1.92854785	1.92854314	1.06428955	1.06429031
2.6	2.88753556	2.88754775	1.91380375	1.91380007	1.06830245	1.06830420
2.8	2.85600966	2.85601747	1.89766815	1.89766599	1.07207186	1.07207558
3	2.82095988	2.82096223	1.88015051	1.88014976	1.07559095	1.07559683
3.2	2.78240780	2.78240495	1.86126545	1.86126546	1.07885301	1.07886049
3.4	2.74039892	2.74039235	1.84103267	1.84103224	1.08185120	1.08185913
3.6	2.69500377	2.69499586	1.81947693	1.81947507	1.08457837	1.08458545
3.8	2.64631866	2.64631227	1.79662803	1.79662425	1.08702703	1.08703230
4	2.59446609	2.59446388	1.77252096	1.77251532	1.08918948	1.08919264
4.2	2.53959459	2.53959849	1.74719607	1.74718962	1.09105803	1.09105968
4.4	2.48187811	2.48188890	1.72069924	1.72069352	1.09262537	1.09262673
4.6	2.42151482	2.42153108	1.69308212	1.69307852	1.09388487	1.09388740
4.8	2.35872541	2.35874312	1.66440224	1.66440096	1.09483099	1.09483549
5	2.29375081	2.29376278	1.63472320	1.63472180	1.09545957	1.09546511

Table 9
Comparison of the results for first three cases based on pray class $q(\tau)$.

τ	Proposed	Adams [55]	Proposed	Adams [55]	Proposed	Adams [55]
	Case 1	Case 1	Case 2	Case 2	Case 3	Case 3
	$q(\tau)$	$q(\tau)$	$q(\tau)$	$q(\tau)$	$q(\tau)$	$q(\tau)$
0	6.00000063	6.00000000	4.00000000	4.00000000	1.99999961	2.00000000
0.2	6.28037341	6.28037774	4.12019638	4.12020988	2.02749211	2.02748884
0.4	6.57462633	6.57462048	4.24405242	4.24406247	2.05556335	2.05556104
0.6	6.88319454	6.88317581	4.37158317	4.37158585	2.08422300	2.08422526
0.8	7.20649278	7.20646379	4.50278685	4.50279913	2.11348721	2.11348987
1	7.54490460	7.54486976	4.63769831	4.63771148	2.14336444	2.14336308
1.2	7.89877252	7.89873643	4.77631752	4.77632151	2.17385870	2.17385287
1.4	8.26838871	8.26835536	4.91861050	4.91861634	2.20497429	2.20496697
1.6	8.65398578	8.65395832	5.06455608	5.06457056	2.23671768	2.23671285
1.8	9.05572757	9.05570807	5.21413023	5.21414625	2.26909734	2.26909767
2	9.47369967	9.47368895	5.36728171	5.36729081	2.30212258	2.30212825
2.2	9.90790002	9.90789885	5.52393560	5.52393824	2.33580225	2.33581105
2.4	10.35822956	10.35823340	5.68400429	5.68400686	2.37014370	2.37015212
2.6	10.82448330	10.82449290	5.84739122	5.84739924	2.40515241	2.40515709
2.8	11.30634210	11.30634942	6.01398806	6.01400305	2.44083203	2.44083102
3	11.80336545	11.80336873	6.18367030	6.18368868	2.47718494	2.47717873
3.2	12.31498554	12.31498244	6.35629423	6.35631032	2.51421304	2.51420414
3.4	12.84050306	12.84049162	6.53169626	6.53170667	2.55191850	2.55191084
3.6	13.37908490	13.37906459	6.70969438	6.70969889	2.59030428	2.59030171
3.8	13.92976414	13.92973671	6.89009066	6.89009278	2.62937431	2.62937891
4	14.49144249	14.49141238	7.07267388	7.07267911	2.66913298	2.66914413
4.2	15.06289533	15.06286848	7.25722132	7.25723270	2.70958424	2.70959794
4.4	15.64277944	15.64276067	7.44349885	7.44351496	2.75073018	2.75074055
4.6	16.22964350	16.22963652	7.63125926	7.63127397	2.79256934	2.79257101
4.8	16.82194105	16.82194451	7.82023885	7.82024594	2.83509502	2.83508777
5	17.41804610	17.41805057	8.01015280	8.01015632	2.87829385	2.87828813

Table 10
Comparison of the results for last three cases based on predator class $p(\tau)$.

τ	Proposed Case 4 $p(\tau)$	Adams [55] Case 4 $p(\tau)$	Proposed Case 5 $p(\tau)$	Adams [55] Case 5 $p(\tau)$	Proposed Case 6 $p(\tau)$	Adams [55] Case 6 $p(\tau)$
0	1.00000001	1.00000000	2.00000001	2.00000000	2.99999934	3.00000000
0.2	1.01168499	1.01166923	2.01189409	2.01190006	3.00039793	3.00038101
0.4	1.02349407	1.02347783	2.02359057	2.02359435	2.99913839	2.99909355
0.6	1.03543782	1.03542732	2.03507361	2.03507356	2.99614167	2.99609394
0.8	1.04752773	1.04751925	2.04632734	2.04632851	2.99137109	2.99134145
1	1.05976366	1.05975510	2.05734636	2.05734986	2.98480342	2.98479864
1.2	1.07214545	1.07213639	2.06812430	2.06812820	2.97641703	2.97643177
1.4	1.08467512	1.08466466	2.07865064	2.07865407	2.96618868	2.96621110
1.6	1.09735493	1.09734145	2.08891427	2.08891792	2.95409415	2.95411123
1.8	1.11018602	1.11016831	2.09890557	2.09891017	2.94011018	2.94011199
2	1.12316860	1.12314679	2.10861591	2.10862122	2.92421657	2.92419746
2.2	1.13630267	1.13627846	2.11803657	2.11804141	2.90639809	2.90635821
2.4	1.14958874	1.14956489	2.12715807	2.12716109	2.88664600	2.88658987
2.6	1.16302821	1.16300766	2.13597013	2.13597061	2.86495904	2.86489423
2.8	1.17662330	1.17660835	2.14446212	2.14446033	2.84134410	2.84127960
3	1.19037691	1.19036857	2.15262346	2.15262062	2.81581644	2.81576073
3.2	1.20429222	1.20428990	2.16044405	2.16044190	2.78839963	2.78835894
3.4	1.21837237	1.21837395	2.16791444	2.16791465	2.75912521	2.75910237
3.6	1.23262014	1.23262233	2.17502584	2.17502943	2.72803214	2.72802620
3.8	1.24703774	1.24703667	2.18176999	2.18177685	2.69516614	2.69517239
4	1.26162659	1.26161856	2.18813886	2.18814767	2.66057885	2.66058954
4.2	1.27638723	1.27636966	2.19412427	2.19413271	2.62432705	2.62433363
4.4	1.29131929	1.29129157	2.19971750	2.19972298	2.58647177	2.58646645
4.6	1.30642144	1.30638593	2.20490882	2.20490960	2.54707748	2.54705672
4.8	1.32169144	1.32165438	2.20968710	2.20968387	2.50621133	2.50617883
5	1.33712615	1.33709856	2.21403933	2.21403733	2.46394242	2.46391314

Table 11
Comparison of the results for last three cases based on pray class $q(\tau)$.

τ	Proposed Case 4 $q(\tau)$	Adams [55] Case 4 $q(\tau)$	Proposed Case 5 $q(\tau)$	Adams [55] Case 5 $q(\tau)$	Proposed Case 6 $q(\tau)$	Adams [55] Case 6 $q(\tau)$
0	2.99999996	3.00000000	5.00000000	5.00000000	7.00000000	7.00000000
0.2	2.99878788	2.99883518	5.04840380	5.04841191	7.19586179	7.19591442
0.4	2.99770923	2.99774116	5.09763794	5.09765330	7.39722580	7.39727875
0.6	2.99669471	2.99671874	5.14771926	5.14773292	7.60408889	7.60411521
0.8	2.99573432	2.99576870	5.19864987	5.19865910	7.81642026	7.81643239
1	2.99484926	2.99489182	5.25043355	5.25044000	8.03420870	8.03422418
1.2	2.99404672	2.99408890	5.30307717	5.30308347	8.25744055	8.25746898
1.4	2.99332366	2.99336076	5.35658918	5.35659716	8.48608633	8.48612850
1.6	2.99267623	2.99270822	5.41097821	5.41098834	8.72009555	8.72014724
1.8	2.99210315	2.99213213	5.46625224	5.46626401	8.95939561	8.95944942
2	2.99160520	2.99163336	5.52241839	5.52243079	9.20389203	9.20394300
2.2	2.99118397	2.99121276	5.57948289	5.57949492	9.45346897	9.45351226
2.4	2.99084102	2.99087123	5.63745122	5.63746230	9.70798950	9.70802312
2.6	2.99057763	2.99060968	5.69632828	5.69633832	9.96729560	9.96731966
2.8	2.99039492	2.99042902	5.75611852	5.75612802	10.23120791	10.23122360
3	2.99029398	2.99033019	5.81682611	5.81683576	10.49952553	10.49953482
3.2	2.99027601	2.99031414	5.87845494	5.87846572	10.77202586	10.77203155
3.4	2.99034234	2.99038183	5.94100867	5.94102124	11.04846466	11.04847000
3.6	2.99049436	2.99053425	6.00449059	6.00450520	11.32857652	11.32858416
3.8	2.99073342	2.99077240	6.06890361	6.06892002	11.61207542	11.61208716
4	2.99106066	2.99109730	6.13424999	6.13426719	11.89865557	11.89867226
4.2	2.99147689	2.99150998	6.20053122	6.20054793	12.18799219	12.18801123
4.4	2.99198249	2.99201149	6.26774768	6.26776249	12.47974202	12.47975965
4.6	2.99257731	2.99260292	6.33589840	6.33591050	12.77354343	12.77355422
4.8	2.99326067	2.99328534	6.40498074	6.40499097	13.06901583	13.06901712
5	2.99403128	2.99405988	6.47499001	6.47500184	13.36575843	13.36575584

5. Concluding remarks

The design of the Gudermannian neural networks is stated for solving the biological predator and prey system, which is based on the system of nonlinear equations. The performances of GNNs are performed effectively with the use of optimization based on global and local search procedures, i.e., GA-IPA. The design of merit function using the differential system of the prey-predator has been presented and optimization is performed based on the computing solver GNNs-GA-IPA. Six dissimilar variants of the prey and predator system have been effectively tested by using the proposed GNNs-GA-IPA. The overlapping of the proposed results through GNNs-GA-IPA and the reference results is performed that indicates the exactness of the proposed scheme. The AE values are found in good measure for each case of both prey and predator system. The plots of weight vectors and numerical formulation have also provided in interval 0 to 5 with 0.2 step size. These statistical performances based on Min, Med and SIR operatives is tabulated for both indexes of each case of the nonlinear prey and predator system. These small values through these statistical gages authenticate the accurateness of designed GNNs-GA-IPA. Moreover, statistical plots Fit, TIC and ENSE together with boxplots/histograms are presented for both indexes of each case of the nonlinear prey and predator system. These statistical performances indicate that most of the trials achieved higher accuracy level for both indexes of each case of the nonlinear prey and predator system.

In future, the other neural networks can be applied to solve the proposed solver is applied to solve the NDPPM [56–58], coronavirus model [59,60], monkeypox virus model [61], chaotic financial model [62], and drug therapy [63].

Data availability

No data was used for the research described in the article.

CRediT authorship contribution statement

Hafsa Alkaabi: Investigation, Formal analysis. **Noura Alkarbi:** Formal analysis, Investigation. **Nouf Almemari:** Formal analysis, Investigation. **Salem Ben Said:** Methodology, Supervision. **Zulqurnain Sabir:** Writing – original draft, Supervision.

Declaration of competing interest

The authors declare that they have no known competing financial interests or personal relationships that could have appeared to influence the work reported in this paper.

Acknowledgement

The authors are thankful to UAEU for the financial support through the SURE Plus grant 2023.

References

[1] B. Ghanbari, et al., Numerical solution of predator-prey model with Beddington-DeAngelis functional response and fractional derivatives with Mittag-Leffler kernel, Chaos: An Interdisciplinary Journal of Nonlinear Science 29 (6) (2019) 063103.
[2] M. Umar, et al., Stochastic numerical technique for solving HIV infection model of CD4+ T cells, The European Physical Journal Plus 135 (5) (2020) 403.
[3] Y.G. Sanchez, et al., Design of a nonlinear SITR fractal model based on the dynamics of a novel coronavirus (COVID), Fractals 28 (2020) 2040026.
[4] A. Mhlanga, A theoretical model for the transmission dynamics of HIV/HSV-2 co-infection in the presence of poor HSV-2 treatment adherence, Applied mathematics and nonlinear sciences 3 (2) (2018) 603–626.
[5] M. Umar, et al., A stochastic computational intelligent solver for numerical treatment of mosquito dispersal model in a heterogeneous environment, The European Physical Journal Plus 135 (7) (2020) 1–23.
[6] J. Biazar, et al., A computational method for solution of the prey and predator problem, Appl. Math. Comput. 163 (2) (2005) 841–847.
[7] F.J. Solis, Self-limitation in a discrete predator–prey model, Math. Comput. Model. 48 (1) (2008) 191–196.
[8] Z. Sabir, T. Botmart, M.A.Z. Raja, W. Weera, An advanced computing scheme for the numerical investigations of an infection-based fractional-order nonlinear prey-predator system, PLoS One 17 (3) (2022) e0265064.
[9] M. Umar, et al., Intelligent computing for numerical treatment of nonlinear prey–predator models, Appl. Soft Comput. 80 (2019) 506–524.
[10] T. Saeed, J.L. Guirao, Z. Sabir, H.H. Alsulami, Y.G. Sánchez, A computational approach to solve the nonlinear biological prey–predator system, Fractals 30 (10) (2022) 2240267.
[11] C.S. Holling, The functional response of invertebrate predators to prey density, Mem. Entomol. Soc. Can. 98 (S48) (1966) 5–86.
[12] M. Danca, et al., Detailed analysis of a nonlinear prey-predator model, J. Biol. Phys. 23 (1997) 11–20.
[13] X. Liu, et al., Complex dynamic behaviors of a discrete-time predator–prey system, Chaos, Solit. Fractals 32 (1) (2007) 80–94.
[14] Z. Jing, et al., Bifurcation and chaos in discrete-time predator–prey system, Chaos, Solit. Fractals 27 (1) (2006) 259–277.
[15] B. Batiha, The solution of the prey and predator problem by differential transformation method, Int. J. Basic Appl. Sci. 4 (1) (2014) 36–43.
[16] S. Paul, et al., Numerical solution of Lotka Volterra prey predator model by using Runge–Kutta–Fehlberg method and Laplace Adomian decomposition method, Alex. Eng. J. 55 (1) (2016) 613–617.
[17] M.R. Garvie, et al., Simple finite element methods for approximating predator–prey dynamics in two dimensions using matlab, Bull. Math. Biol. 77 (3) (2015) 548–578.
[18] J. Yu, et al., Homotopy analysis method for a prey-predator system with holling IV functional response, Appl. Mech. Mater. 687-691 (2014) 1286–1291, https://doi.org/10.4028/www.scientific.net/AMM.687-691.1286.
[19] N. Bildik, et al., The use of Sumudu decomposition method for solving predator-prey systems, Mathematical Sciences Letters 5 (3) (2016) 285–289.
[20] S.S. Ray, A new coupled fractional reduced differential transform method for the numerical solution of fractional predator-prey system, Comput. Model. Eng. Sci.: Comput. Model. Eng. Sci. 105 (3) (2015) 231–249.
[21] I. Gad, et al., The Solution of Fractional Order Epidemic Model by Implicit Adams Methods, 2015.
[22] S. Mall, et al., Application of Legendre Neural Network for solving ordinary differential equations, Appl. Soft Comput. 43 (2016) 347–356.

[23] Z. Sabir, et al., Heuristic computing technique for numerical solutions of nonlinear fourth order Emden–Fowler equation, Math. Comput. Simulat. 178 (2020) 534–548.
[24] M.K. Ammar, et al., Calculation of line of site periods between two artificial satellites under the action air drag, Applied Mathematics and Nonlinear Sciences 3 (2) (2018) 339–352.
[25] K. Nisar, et al., Design of morlet wavelet neural network for solving a class of singular pantograph nonlinear differential models, IEEE Access (2021), https://doi.org/10.1109/ACCESS.2021.3072952.
[26] M.K. Ammar, et al., Visibility intervals between two artificial satellites under the action of Earth oblateness, Applied Mathematics and Nonlinear Sciences 3 (2) (2018) 353–374.
[27] Z. Sabir, N. Akkurt, S.B. Said, A novel radial basis Bayesian regularization deep neural network for the Maxwell nanofluid applied on the Buongiorno model, Arab. J. Chem. 16 (6) (2023) 104706.
[28] Z. Sabir, S.B. Said, Heuristic computing for the novel singular third order perturbed delay differential model arising in thermal explosion theory, Arab. J. Chem. 16 (3) (2023) 104509.
[29] M. Umar, et al., Integrated neuro-swarm heuristic with interior-point for nonlinear SITR model for dynamics of novel COVID-19, Alex. Eng. J. 60 (3) (2021) 2811–2824.
[30] M. Umar, et al., A stochastic intelligent computing with neuro-evolution heuristics for nonlinear SITR system of novel COVID-19 dynamics, Symmetry 12 (10) (2020) 1628.
[31] Z. Sabir, et al., Integrated intelligent computing paradigm for nonlinear multi-singular third-order Emden–Fowler equation, Neural Comput. Appl. 33 (8) (2021) 3417–3436.
[32] Z. Sabir, et al., Design of neuro-swarming-based heuristics to solve the third-order nonlinear multi-singular Emden–Fowler equation, The European Physical Journal Plus 135 (5) (2020) 410.
[33] Z. Sabir, S.B. Said, J.L. Guirao, A radial basis scale conjugate gradient deep neural network for the monkeypox transmission system, Mathematics 11 (4) (2023) 975.
[34] M.A.Z. Raja, et al., A new stochastic computing paradigm for the dynamics of nonlinear singular heat conduction model of the human head, The European Physical Journal Plus 133 (9) (2018) 364.
[35] Z. Sabir, et al., Evolutionary computing for nonlinear singular boundary value problems using neural network, genetic algorithm and active-set algorithm, The European Physical Journal Plus 136 (2) (2021) 1–19.
[36] Z. Sabir, S.B. Said, Q. Al-Mdallal, A fractional order numerical study for the influenza disease mathematical model, Alex. Eng. J. 65 (2023) 615–626.
[37] Z. Sabir, R. Sadat, M.R. Ali, S.B. Said, M. Azhar, A numerical performance of the novel fractional water pollution model through the Levenberg-Marquardt backpropagation method, Arab. J. Chem. 16 (2) (2023) 104493.
[38] M. Umar, et al., A stochastic numerical computing heuristic of SIR nonlinear model based on dengue fever, Results Phys. 19 (2020) 103585.
[39] H. Liang, et al., An improved genetic algorithm optimization fuzzy controller applied to the wellhead back pressure control system, Mech. Syst. Signal Process. 142 (2020) 106708.
[40] N. Metawa, et al., Genetic algorithm based model for optimizing bank lending decisions, Expert Syst. Appl. 80 (2017) 75–82.
[41] S. Sayed, et al., A nested genetic algorithm for feature selection in high-dimensional cancer microarray datasets, Expert Syst. Appl. 121 (2019) 233–243.
[42] C.H. Chou, et al., Hybrid genetic algorithm and fuzzy clustering for bankruptcy prediction, Appl. Soft Comput. 56 (2017) 298–316.
[43] I. do Valle Tomaz, et al., Investigations on quality characteristics in gas tungsten arc welding process using artificial neural network integrated with genetic algorithm, Int. J. Adv. Des. Manuf. Technol. 113 (11) (2021) 3569–3583.
[44] P.A.A. Resende, et al., Adaptive anomaly-based intrusion detection system using genetic algorithm and profiling, Security and Privacy 1 (4) (2018) e36.
[45] M. Elhoseny, et al., Bezier curve based path planning in a dynamic field using modified genetic algorithm, Journal of Computational Science 25 (2018) 339–350.
[46] F. Millo, et al., Optimization of automotive diesel engine calibration using genetic algorithm techniques, Energy 158 (2018) 807–819.
[47] T. Zhang, et al., Control of a novel synthetical index for the local indoor air quality by the artificial neural network and genetic algorithm, Sustain. Cities Soc. 51 (2019) 101714.
[48] S. Tiachacht, et al., Damage assessment in structures using combination of a modified Cornwell indicator and genetic algorithm, Eng. Struct. 177 (2018) 421–430.
[49] J. Wambacq, et al., Interior-point methods for the phase-field approach to brittle and ductile fracture, Comput. Methods Appl. Mech. Eng. 375 (2021) 113612.
[50] A. Zanelli, et al., Forces nlp: an efficient implementation of interior-point methods for multistage nonlinear nonconvex programs, Int. J. Control 93 (1) (2020) 13–29.
[51] M. Stefanova, et al., An interior-point method-based solver for simulation of aircraft parts riveting, Eng. Optim. 50 (5) (2018) 781–796.
[52] C. El Boustani, et al., Extending interior-point methods to nonlinear second-order cone programming: application to finite-strain elastoplasticity, Int. J. Numer. Methods Eng. 122 (1) (2021) 270–293.
[53] M.C. Corbineau, et al., PIPA: a new proximal interior point algorithm for large-scale convex optimization, April, in: 2018 IEEE International Conference on Acoustics, Speech and Signal Processing (ICASSP), IEEE, 2018, pp. 1343–1347.
[54] J. Chen, et al., A united framework with multi-operator evolutionary algorithms and interior point method for efficient single objective optimisation problem solving, Int. J. High Perform. Comput. Netw. 13 (3) (2019) 340–353.
[55] M. Umar, Z. Sabir, M.A.Z. Raja, F. Amin, T. Saeed, Y.G. Sanchez, Design of intelligent computing solver with Morlet wavelet neural networks for nonlinear predator–prey model, Appl. Soft Comput. 134 (2023) 109975.
[56] Yurong Liu, et al., Exponential stability of Markovian jumping Cohen-Grossberg neural networks with mixed mode-dependent time-delays, Neurocomputing 177 (2016) 409–415.
[57] B. Du, et al., Existence and asymptotic behavior results of periodic solution for discrete-time neutral-type neural networks, J. Franklin Inst. 353 (2) (2016) 448–461.
[58] Elbaz I. Abouelmagd, et al., Reduction the secular solution to periodic solution in the generalized restricted three-body problem, Astrophys. Space Sci. 350 (2) (2014) 495–505.
[59] W. Adel, Y.A. Amer, E.S. Youssef, A.M. Mahdy, Mathematical analysis and simulations for a Caputo-Fabrizio fractional COVID-19 model, Partial Differential Equations in Applied Mathematics 8 (2023) 100558.
[60] N. Ahmed, A. Elsonbaty, A. Raza, M. Rafiq, W. Adel, Numerical simulation and stability analysis of a novel reaction–diffusion COVID-19 model, Nonlinear Dynam. 106 (2021) 1293–1310.
[61] A. El-Mesady, W. Adel, A.A. Elsadany, A. Elsonbaty, Stability analysis and optimal control strategies of a fractional-order monkeypox virus infection model, Phys. Scripta 98 (9) (2023) 095256.
[62] W. Weera, T. Botmart, C. Chantawat, Z. Sabir, W. Adel, M.A.Z. Raja, M. Kristiawan, An intelligence computational approach for the fractional 4D chaotic financial model, Comput. Mater. Continua (CMC) 74 (2) (2023).
[63] N. Ahmed, A. Elsonbaty, W. Adel, D. Baleanu, M. Rafiq, Stability analysis and numerical simulations of spatiotemporal HIV CD4+ T cell model with drug therapy, Chaos: An Interdisciplinary Journal of Nonlinear Science 30 (8) (2020).